

Fall 1-31-1995

Time domain and frequency domain analysis of myoelectric signals during muscle fatigue

Rakesh M. Maniar
New Jersey Institute of Technology

Follow this and additional works at: <https://digitalcommons.njit.edu/theses>



Part of the [Biomedical Engineering and Bioengineering Commons](#)

Recommended Citation

Maniar, Rakesh M., "Time domain and frequency domain analysis of myoelectric signals during muscle fatigue" (1995). *Theses*. 1146.

<https://digitalcommons.njit.edu/theses/1146>

This Thesis is brought to you for free and open access by the Electronic Theses and Dissertations at Digital Commons @ NJIT. It has been accepted for inclusion in Theses by an authorized administrator of Digital Commons @ NJIT. For more information, please contact digitalcommons@njit.edu.

Copyright Warning & Restrictions

The copyright law of the United States (Title 17, United States Code) governs the making of photocopies or other reproductions of copyrighted material.

Under certain conditions specified in the law, libraries and archives are authorized to furnish a photocopy or other reproduction. One of these specified conditions is that the photocopy or reproduction is not to be “used for any purpose other than private study, scholarship, or research.” If a user makes a request for, or later uses, a photocopy or reproduction for purposes in excess of “fair use” that user may be liable for copyright infringement,

This institution reserves the right to refuse to accept a copying order if, in its judgment, fulfillment of the order would involve violation of copyright law.

Please Note: The author retains the copyright while the New Jersey Institute of Technology reserves the right to distribute this thesis or dissertation

Printing note: If you do not wish to print this page, then select “Pages from: first page # to: last page #” on the print dialog screen

The Van Houten library has removed some of the personal information and all signatures from the approval page and biographical sketches of theses and dissertations in order to protect the identity of NJIT graduates and faculty.

ABSTRACT

TIME DOMAIN AND FREQUENCY DOMAIN ANALYSIS OF MYOELECTRIC SIGNALS DURING MUSCLE FATIGUE.

by
Rakesh M. Maniar

Spectral analysis of the EMG signal is a useful tool for studying the complex phenomena of fatigue. The spectral parameters of mean frequency and median frequency, and the time domain parameter of root mean square have been used to measure localized fatigue.

The normal values of median frequency and its decline with fatigue have not as yet been determined in healthy subjects. This should be done in order to apply spectral analysis for clinical evaluations of abnormal populations. Normal median frequency values and its slope were established in this work for the upper extremity muscles of biceps, triceps and deltoid during a pilot study. The result showed that the triceps has a lower slope value, hence more type I fiber (fatigue resistant) as compared to that of biceps and deltoids. In addition, a monopolar fine wire electrode referenced to a surface electrode was compared with a bipolar surface electrode and bipolar fine wire electrodes in order to test the monopolar fine wire electrode as a technique to measure fatigue. The result showed that the monopolar fine wire electrode measured fatigue more reliably than the surface electrode. Further, for bipolar fine wire electrodes, where the active electrode is proximal to the motor point, the distance between the active electrode and the reference electrode is important in order to measure fatigue reliably.

**TIME DOMAIN AND FREQUENCY DOMAIN ANALYSIS OF
MYOELECTRIC SIGNALS DURING MUSCLE FATIGUE**

by
Rakesh M. Maniar

**A Thesis
Submitted to the Faculty of
New Jersey Institute of Technology
in Partial Fulfillment of the Requirements for the Degree of
Master of Science in Biomedical Engineering**

Biomedical Engineering Committee

January 1995

Blank Page

APPROVAL PAGE

**TIME DOMAIN AND FREQUENCY DOMAIN ANALYSIS OF
MYOELECTRIC SIGNALS DURING MUSCLE FATIGUE**

Rakesh M. Maniar

Dr. Stanley Reisman, Thesis Advisor
Professor of Electrical Engineering and Associate
Chairperson of Graduate Studies, NJIT

Date

Dr. David Kristol, Committee Member
Professor of Chemistry and Director of
Biomedical Engineering Program, NJIT

Date

Dr. Thomas W. Findley, Committee Member
Associate Professor of Medicine, UMDNJ
Director of Research, Kessler Institute for
Rehabilitation

Date

BIOGRAPHICAL SKETCH

Author: Rakesh M. Maniar

Degree: Master of Science in Biomedical Engineering

Place of Birth: Jamnagar, Gujarat, India

Undergraduate and Graduate Education:

- Master of Science in Biomedical Engineering,
New Jersey Institute of Technology, Newark, NJ, 1995
- Post Graduate Diploma in Medical Instrumentation Technology,
Bharathiar University, Coimbatore, TN, India, 1991
- Bachelor of Science in Instrumentation and Control Engineering,
Bharathiar University, Coimbatore, TN, India, 1990

Major: Biomedical Engineering

This thesis is dedicated to my beloved parents,
Rashmi and Mahesh Maniar
and also families of
Maniar, Parekh and Mehta.

ACKNOWLEDGMENT

The author wishes to express his sincere gratitude to his advisor, Dr. Stanely Reisman, for his guidance, friendship, and moral support throughout this research.

Special thanks to Dr. David Kristol and Dr. Thomas Findley for serving as member of the committee.

The author is especially grateful to Dr. Lisa Krivickas, Dr. Brian Davis and Dr. Andre' Taylor, who gave the author the opportunity to work with them on their research project and provided valuable medical information.

The author appreciates the help and suggestions from John Andrews.

And finally, a thank you to the entire research department of the Kessler Institute for Rehabilitation for their help.

TABLE OF CONTENTS

Chapter	Page
1 BACKGROUND.....	1
1.1 Introduction.....	1
1.2 Contraction of Skeletal Muscle.....	2
1.2.1 Physiologic Anatomy of Skeletal Muscle.....	2
1.2.2 The Motor Unit.....	6
1.2.3 Resting and Action Potential.....	7
1.2.4 Mechanism of Muscle Contraction.....	9
1.2.5 Energetics of Muscle Contraction.....	12
1.3 Anatomical Guide of Muscles Under Study.....	13
1.3.1 Biceps Brachii.....	14
1.3.2 Triceps: Lateral Head.....	15
1.3.3 Deltoid: Middle Head.....	16
1.4 Electromyogram.....	16
1.5 Fatigue.....	18
1.6 Mathematical Techniques.....	20
1.7 Statistical Techniques.....	24
1.8 Scope of the Thesis.....	27
1.8.1 Objective and Literature Review of Group 1.....	27
1.8.2 Objective and Literature Review of Group 2.....	31
1.9 Body Fat Estimation.....	33

TABLE OF CONTENTS
(Continued)

Chapter	Page
2 METHODS.....	35
2.1 Experimental Setup for Group I.....	35
2.1.1 Electrode Placement and Mounting.....	36
2.1.2 Testing Protocol.....	37
2.2 Experimental Setup for Group II.....	38
2.2.1 Electrode Placement and Mounting.....	38
2.2.2 Testing Protocol.....	40
2.3 Data Acquisition for Group I.....	40
2.4 Data Acquisition for Group II.....	42
2.5 Data Analysis for Group I.....	43
2.6 Data Analysis for Group II.....	45
3 RESULTS.....	49
3.1 Results of Group I.....	49
3.1.1 Comparison of Delsys and Teca Surface EMG Electrode.....	49
3.1.2 Experimental Results.....	51
3.2 Results of Group II.....	55
4 DISCUSSION AND CONCLUSIONS.....	59
4.1 Discussion and Conclusions for Group I.....	59
4.2 Discussion and Conclusions for Group II.....	63

TABLE OF CONTENTS
(Continued)

Chapter	Page
4.3 Suggestions for Future Work.....	67
APPENDIX A Tables of Median Frequency, Mean Frequency and RMS Values.....	69
APPENDIX B Instrumentation.....	76
APPENDIX C Data Acquisition.....	82
APPENDIX D Flow Chart and Programming Details.....	85
APPENDIX E Power Analysis.....	99
REFERENCES.....	102

LIST OF TABLES

Table	Page
1.1 Body fat norms.....	34
2.1 Electrode configurations used for group II.....	41
3.1 Delsys™ vs Teca™ with regards to initial median frequency.....	50
3.2 Linear regression and correlation parameters for 3 muscles.....	52
3.3 Range of normal median frequency values for 3 muscles.....	54
3.7 Range of values of y intercept and slopes of median frequency and mean frequency.....	56
4.1 Slope, y intercept and correlation coefficient of median frequency.....	66
3.4 Slope, y intercept and correlation coefficient of median frequency for group II...70	
3.5 Slope, y intercept and correlation coefficient of mean frequency for group II.....72	
3.6 Slope, y intercept and correlation coefficient of root mean square for group II.....	74
E.1 Sample size for common values of W/S.....	101
E.2 Sample size for revealing a correlation.....	102

LIST OF FIGURES

Figure	Page
1.1 Organization of skeletal muscle from the gross to myofibril level.....	3
1.2 A myofibril and its components; the actin filaments and the myosin filaments.....	3
1.3 The myosin filament.....	5
1.4 The actin filament.....	5
1.5 Scheme of a motor unit.....	6
1.6 A typical action potential.....	9
1.7 The relax and contracted states of a myofibril, showing sliding of the actin filaments into the spaces between the myosin filaments.....	11
1.8 The “walk-along” mechanism for contraction of the muscle.....	11
1.9 The biceps brachii.....	14
1.10 Triceps lateral head.....	15
1.11 Deltoid: Middle head.....	16
1.12 A typical EMG signal recorded from biceps brachii using surface electrode.....	19
1.13 Shows spectrum of biceps brachii before and during fatigue.....	19
1.14 Computational parts of the processing system.....	23
1.15 Shows meaning of linear regression parameters.....	26
1.16 Location of skin fold measurements in male subjects.....	34
2.1 Electrode placement on the distal upper arm.....	39
2.2 Block diagram of instrumentation system common to both the projects except for the transducer which was used only group I.....	48
3.1 Shows the comparison of the Delsys with the Teca surface EMG electrode	51

LIST OF FIGURES
(continued)

Figure	Page
3.2 Shows EMG and the force level maintained at 50% MVC.....	53
3.3 Shows least squares fit to median frequency data: good fit subject 5, biceps, trial 2.....	53
3.4 Least square fit to median frequency and mean frequency data: good fit subject 1, trial 1 monopolar fine wire electrode	56
3.5 Least square fit to rms data: good fit and to median frequency data: poor fit.....	57
4.1 Shows flow chart for processing force.....	62
4.2 Shows large Variations in force maintained at 50% MVC and corresponding least square fit.....	68
B.1 Shows <i>DelsysTM</i> electrode.....	77
B.2 Shows the isolation pre amplifier (Gould #11-5407-59).....	78
B.3. Gould universal amplifier (13-4615-58) and isolated preamp connections.....	79
B.4 Sensotech's Load cell.....	80
B.5 Lange skinfold caliper and in use.....	81
D.1 Shows the flow chart of the software tool developed for group I.....	86
D.2 Shows the flow chart of the software developed for Group II.....	92

CHAPTER 1

BACKGROUND

1.1 Introduction

As the population of the world increases, the need for health care increases. Recently tremendous progress has been made in medical care, especially in such fields as neurology, cardiology and rehabilitation medicine. A major reason for this phenomenal progress has been the union of two important disciplines: engineering and medicine, giving a new interdisciplinary field-biomedical engineering.

There are similarities as well differences between these two disciplines, but there is no doubt that interaction between them has produced wonderful results. The field of biomedical engineering is broad. It encompasses people engaged in a wide spectrum of activities from the basic maintenance of either the body, or a piece of equipment, to research on the frontiers of knowledge in each field [8].

One such interaction between the medicine and engineering is in the area of digital signal processing of physiological signals like the electromyogram (EMG), electrocardiogram (EKG), and electroencephalogram (EEG). This work documents the digital signal processing tool developed and applied to the study of the myoelectric signal (EMG) for two ongoing research projects on the fatigue studies of muscles at the Kessler Institute for Rehabilitation.

1.2 Contraction of Skeletal Muscle

1.2.1 Physiologic Anatomy of Skeletal Muscle

A skeletal muscle, usually referred to as a “muscle,” is primarily a collection of striated muscle fibers bound together and surrounded by connective tissue; the tendons by which it is attached and the branches of blood vessels and nerves within it are also a part of the organ.

All skeletal muscles are made of numerous fibers ranging between 10 and 80 μ m in diameter. They extend the entire length of the muscle. Each fiber is innervated at its middle by only one nerve ending, whose body is in the anterior horn cell of the spinal cord. This termination of the nerve ending of the muscle fiber defines an area known as the endplate region.

Each muscle fiber has a sarcolemma, myofibrils, sarcoplasm, and sarcoplasmic reticulum. The cell membrane of the fiber is called the sarcolemma. The sarcolemma has a thin outer layer that contains numerous thin collagen fibrils. These collagen fibrils fuse with a tendon fiber at the end of the muscle fiber. Many such tendon fibers join together to form the muscle tendons which insert into bones.[19]

Many myofibrils bundle together to form a muscle fiber as shown in Figure 1.1. Each myofibril has about 1500 myosin filaments and 3000 actin filaments. These two types of filaments are responsible for the muscle contraction. These filaments are shown in Figure 1.2.

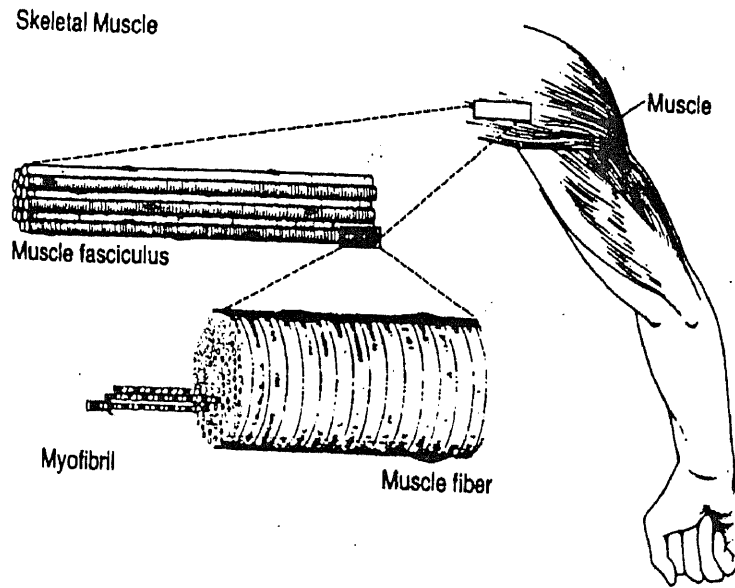


Figure 1.1 Organization of skeletal muscle from the gross to myofibril level.

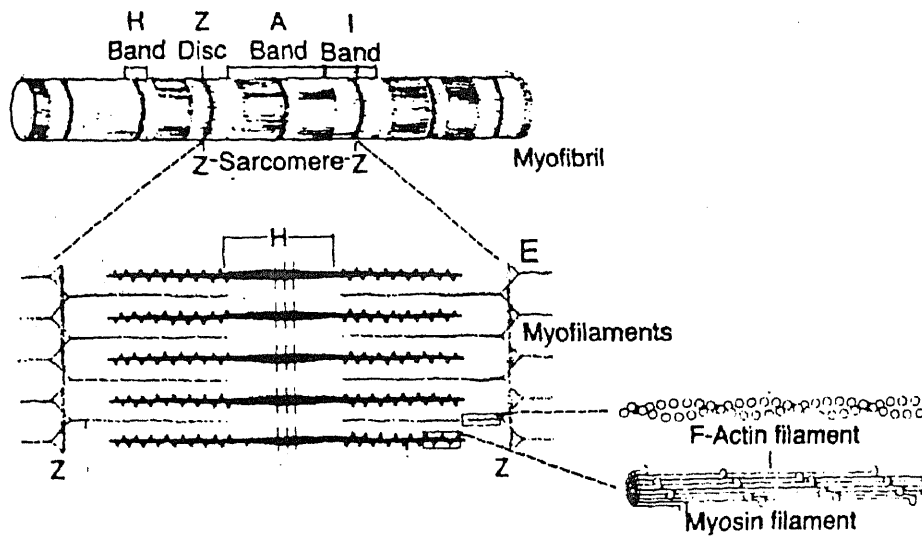


Figure 1.2 A myofibril and its components; the actin filaments and the myosin filaments.

The thick filaments and the thin filaments in the diagram are myosin and actin, respectively. They interdigitate, thereby causing alternate light and dark bands on the myofibrils, hence the striated appearance of the skeletal muscle. The light bands are called I band as they are isotropic to polarized light and contain only the actin filaments. The dark bands contain the myosin filaments as well as the ends of actin filaments. They are called A bands as they are anisotropic to polarized light.

There are numerous small projection from the sides of the myosin filaments called cross-bridges, except in the center of the filaments. They play an important role in the muscle contraction by interacting with the actin filaments. As shown in Figure 1.2 the actin filament extends in both directions from the Z discs to interdigitate with the myosin filaments. The portion between the two Z discs is called a sarcomere. The myofibrils are suspended in the matrix inside the fiber and this matrix is known as sarcoplasm. Besides ions, such as potassium, magnesium, and phosphate; and protein enzymes, sarcoplasm contains endoplasmic reticulum called sarcoplasmic reticulum in the muscle fiber. It plays a significant role in the control system of the muscle contraction.

Figure 1.3. A, illustrates an individual myosin molecule and Figure 1.3. B, illustrates the organization of the molecules to form a myosin filament and as well as its interaction with ends of two actin filaments on one side.

Figure 1.4 clearly shows the actin filament that is composed of two helical strands of F-actin and tropomyosin molecules that fit loosely in grooves between the actin strands. To one end of each tropomyosin molecule is attached a troponin complex that

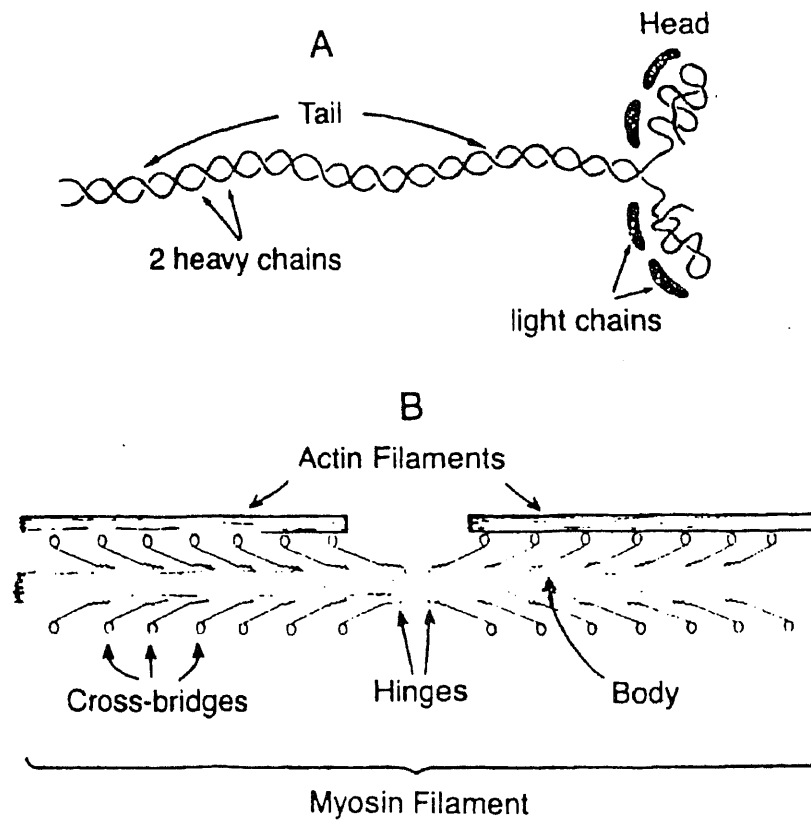


Figure 1.3 A, The myosin molecule. B, Combination of many myosin molecules to form a myosin filament. Also shown interaction between the heads of the cross-bridges and adjacent actin filaments.

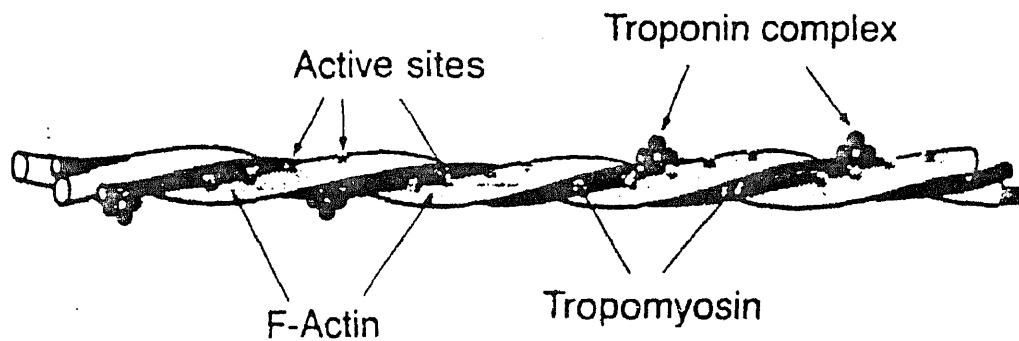


Figure 1.4 The actin filament.

initiates contraction. In the resting state, the tropomyosin lies on the top of the active sites of the actin strands to prevent attraction between the actin and myosin filaments. [19]

1.2.2 The Motor Unit

As described in the previous section, in the normal mammalian skeletal muscle, the fibers never contract individually but in small groups. A group of muscle fibers is innervated by the terminal branches of one nerve axon whose cell body is in the anterior horn of the spinal grey matter. This cell body, its axon and all the muscle fibers it innervates comprise a single motor unit as shown in Figure 1.5

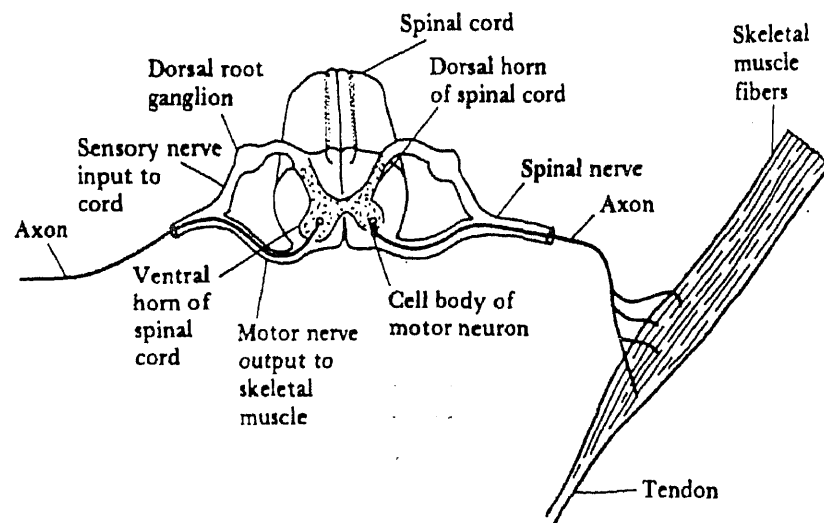


Figure 1.5 Scheme of a motor unit.

This unit is the functional unit of the striated muscle. An impulse propagating down the motoneuron causes almost simultaneous contraction of all the muscle fibers in one motor

unit. The number of muscle fibers that are innervated by one axon varies significantly. The muscles controlling the fine movements and adjustments have the smallest number of muscle fibers per motor unit and the large coarse-contracting muscles have larger motor units.

There also exists a hierarchical arrangement of motor unit sizes within the muscles. The motor units that have smaller numbers of muscle fibers are supplied by the smaller alpha motoneurons. These are the first ones to be excited during a contraction requiring a progressively increasing force. Larger motor units are innervated by larger alpha motoneurons and become activated at progressively higher force level [1]. Motor units are recruited in order of size with the smallest ones being recruited first. In addition type I are recruited before type II..

1.2.3 Resting and Action Potential

The muscle and nerve cells are encapsulated in a semipermeable membrane that permits some substances to selectively pass through the membrane. These cells as described in section 1.3.1 are surrounded by the body fluids. These fluids are conductive solutions containing charged atoms known as ions. The principal ions are sodium (Na^+), potassium (K^+), and chloride (Cl^-). The resting cells allow easy entry of chloride and potassium ions but effectively block the entry of sodium ions.[8]

Since the ions seek a balance between the inside of the cell and the outside, both according to concentration and electric charge, the inability of the sodium to enter the membrane results in two conditions.

1. The outside of the cell becomes more positive than inside because of high concentration of positively charged sodium ions.
2. In order to balance the electric charge, additional potassium ions enter the cell, causing a higher concentration of potassium on the inside than on the outside.

Equilibrium is reached with a potential difference across the membrane, with negative inside and positive on the outside. This membrane potential is called the resting potential. As measurements of the membrane potential is made from inside the cell with respect to the body fluids, the resting potential of a cell is given as negative. The reported measured membrane potential in various cells varies from -60 to -100 mV. A cell in the resting state is known as polarized.

When a section of the cell membrane is stimulated by the flow of ionic current or by some externally applied energy, the characteristic of the membrane changes which allows some of the sodium ions to enter. This entry of sodium ions constitutes an ionic current flow which further reduces the resistance of the membrane to the sodium ions. This results in an avalanche effect in which sodium ions rushes to try to reach a balance with the ions outside. At the same time potassium ions which are at higher concentration inside try to leave the cell but are unable to move as fast as the sodium ions. The net result is that the cell has a positive potential on the inside due to the imbalance of potassium ions. This potential is known as the action potential and is approximately +20 mV. An excited cell which displays an action potential is said to be depolarized.

Once a new state of equilibrium is reached, the ionic currents that reduced the barrier to sodium ions cease and the membrane comes back to its original selectively

permeable condition. The sodium ions are quickly transported to the outside of the cell by an active process called the sodium-potassium pump. The cell becomes repolarized returning back to its resting potential.

Figure 1.6 shows an action-potential waveform, starting at the resting potential, depolarizing and coming back to the resting potential after repolarization. The time scale for the action potential depends on the type of cell producing the potential. In nerve and muscle cells, repolarization occurs very rapidly so that the action potential appears as a spike of as little as 1 msec total duration.

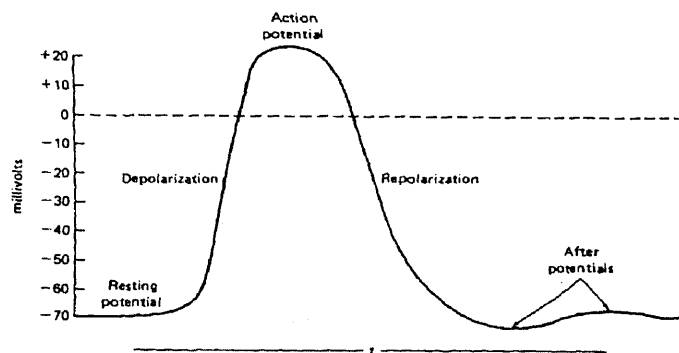


Figure 1.6 A typical action potential.

1.2.4 Mechanism of Muscle Contraction

The initiation and the execution of muscle contraction takes place in the following manner

1. An action potential travels along a motor nerve to its endings on muscle fibers. Acetylcholine, a neurotransmitter, is released by the nerve at its ending.

2. Acetylcholine acts on multiple receptor gated protein channels and causes them to open.
3. Large quantities of sodium ions flow into the muscle fiber membrane through the opened channels, thereby, initiating an action potential.
4. The muscle membrane depolarizes as the action potential travels along the membrane and deeply within the muscle fiber.
5. Inside the muscle fiber the action potential causes the sarcoplasmic reticulum to release large quantities of stored calcium ions.
6. This calcium in turn causes the actin and myosin filaments to slide together by the initiation of attractive forces between them. This is the contractile process and is shown in figure 1.7.
7. The muscle contraction stops after a fraction of a second as the calcium ions are pumped back into the reticulum.
8. Maximum contraction occurs when there is maximum overlap of the actin and cross-bridges of the myosin filaments.

This interaction between the “activated” actin filaments and the myosin cross-bridges has been explained by the “Walk-Along” theory of contraction [19]. Figure 1.8 shows the walk-along mechanism for the muscle contraction. As shown in the figure the head of two cross-bridges attach and release from the active site of the actin filament, and it has been postulated that:

- The attachment of the head of the cross-bridge to an active site simultaneously causes changes in the intramolecular forces between the head and arm of the cross-

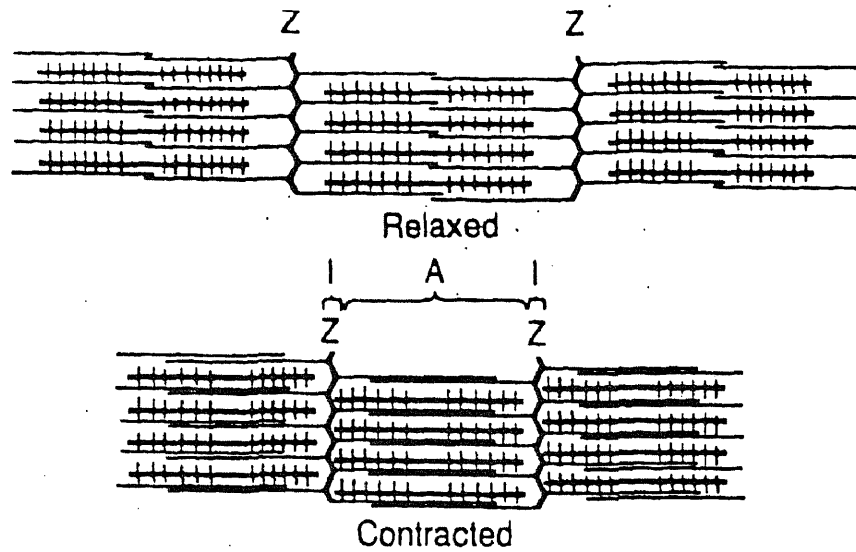


Figure 1.7 The relaxed and contracted states of a myofibril, showing sliding of the actin filaments into the spaces between the myosin filaments.

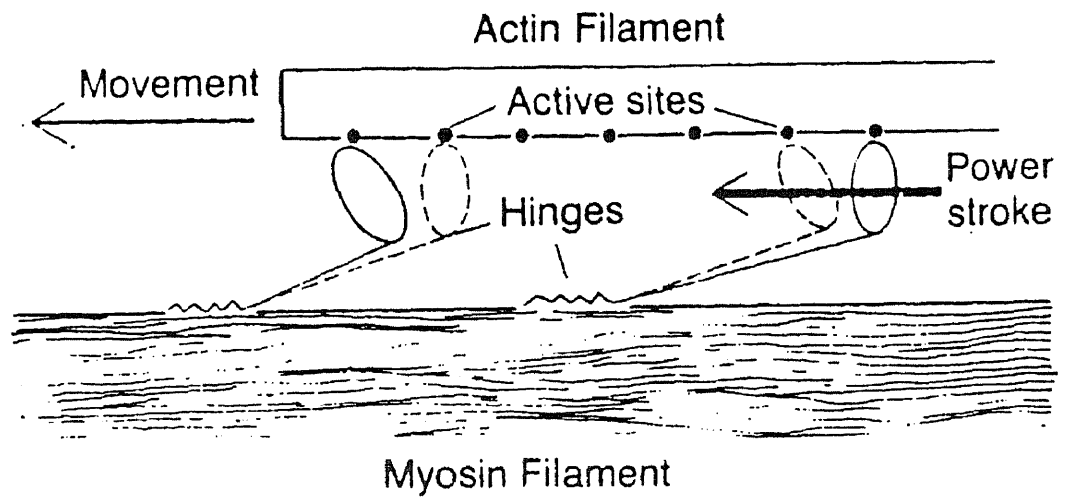


Figure 1.8 The "walk-along" mechanism for contraction of the muscle.

bridge. This new alignment of forces causes the head to bend toward the arm and to drag the actin filament along with it. This bending of the head is called the power stroke.

- The head automatically breaks away from the active site immediately after bending.
- The head then returns back to its original perpendicular position and combines with a new active site farther down along the actin filament.
- The head bends again to cause a new power stroke and the actin filament moves further. This step cycle is repeated.
- The force of contraction is directly proportional to the number of cross bridges. [19]

1.2.5 Energetics of Muscle Contraction

Muscle performs work when it contracts against a load. This implies that energy is transferred from the muscle to the external load. Mathematically, work is defined by

$$W = L \times D \quad (1.1)$$

Where 'W' is the work output.

'L' is the load.

'D' is the distance of movement against the load.

The energy that is required to perform the work is obtained from the chemical reactions that take place in the muscle cell during contraction and this source of energy is adenosine triphosphate (ATP).

During contraction ATP is broken into adenosine diphosphate (ADP). The ADP is rephosphorylated to form new ATP within a fraction of a second and the sources of energy for this rephosphorylation are phosphocreatine, glycogen and oxidative metabolism (combining of oxygen and various cellular foodstuffs to liberate ATP, the main supplier of energy).

The efficiency of the muscle contraction is the percentage of energy input that can be converted into work instead of heat and in muscles it is less than 20-25%. This is because 50% of the energy in foodstuff is lost during the formation of ATP.

Muscle contractions can be classified as isometric, isotonic, and isokinetic. During isometric contraction muscles do not change length. During isotonic contraction the muscle shortens (concentric) or lengthens (eccentric) with tension on the muscle remaining constant and during isokinetic contraction the velocity of contraction remains constant.[19]

1.3 Anatomical Guide of Muscles Under Study

The most commonly tested muscles in clinical EMG are the biceps brachii, triceps and deltoid. When screening for cervical radiculopathy (pinched nerve at the neck) these muscles are often used to evaluate the fifth cervical root (deltoid), sixth cervical root (biceps) and seventh cervical nerve root (triceps). Hence these muscles were of interest for this study. It becomes important to understand the innervation, the origin, the insertion, the position, the electrode insertion site, and the standard manual testing procedure of these muscles.

1.3.1 Biceps Brachii

This muscle is innervated by the musculocutaneous nerve which contains contribution from the fifth and the sixth cervical nerve root. The long head of this muscle originates from the spraglenoid tuberosity of the scapula and the short head arises from the coracoid process of the scapula. Both heads insert on the bicipital tuberosity of the radius.

This muscle can be palpated with the subject in a supine position with arm extended. The best electrode insertion site is into the bulk of the muscle in mid-arm marked X as shown in Figure 1.9. The test maneuver, that is, the standard manual testing procedure to cause voluntary contraction for this muscle, is to flex or supinate the forearm [13].

BICEPS BRACHII

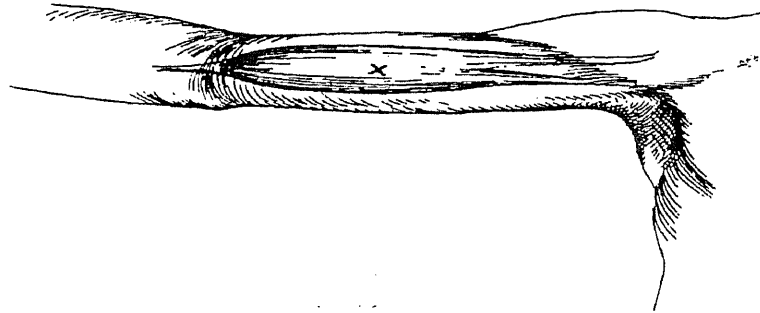


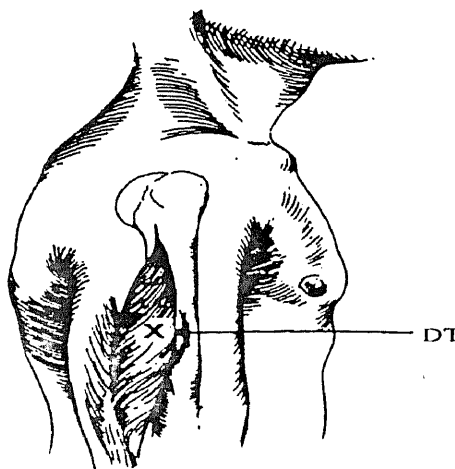
Figure 1.9 The biceps brachii. The electrode insertion site is shown by X.

1.3.2 Triceps: Lateral Head

The triceps lateral head is supplied by the radial nerve which receives contributions from the seventh and the eighth cervical nerve roots, and the first thoracic root. This muscle originates from the dorsal surface of the humerus above the groove for the radial nerve and inserts into the distal aspect of the olecranon process.

This muscle can be felt with the subject in a prone position with arm abducted. The suggested electrode placement site is immediately posterior to the insertion of the deltoid or deltoid tubercle (DT). The placement site is shown as X in Figure 1.10. This muscle can be tested by extension of the elbow.[13].

TRICEPS



Lateral Head

Figure 1.10 Triceps lateral head. The electrode insertion site is shown by X. DT is deltoid tubercle.

1.3.3 Deltoid: Middle Head

The middle head of the deltoid muscle is supplied by the axillary nerve which arises from the fifth and the sixth cervical nerve root. Its origin is from the acromion and insertion is into the deltoid tubercle of the humerus.

This muscle can be palpated with the subject in a supine position with the arm at the side and the electrode placement site (X) is halfway between the tip of the acromion (A) and the deltoid tubercle (DT) as shown in Figure 1.11. The test maneuver for this muscle is the abduction of the arm.[13]

DELTOID, MIDDLE

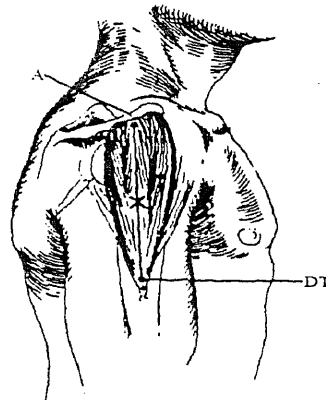


Figure 1.11 Deltoid: Middle head. X is the electrode placement site; A is the acromion process and DT is the deltoid tubercle.

1.4 Electromyogram

Electromyographic (EMG) signals are an indication of the electrical activity of muscles which arise whenever there is a voluntary or involuntary activity of a muscle [29]. The

bioelectric potentials associated with muscle activity may be measured at the surface of the body near a muscle of interest or directly from the muscle by penetrating the skin with needle or fine wire electrodes. As most of the EMG measurements are intended to obtain an indication of the amount of activity of a given muscle, or group of muscles, rather than an individual muscle fiber, the pattern is usually a summation of the individual action potentials from the fibers forming the muscle being examined.

An action potential of a muscle has a fixed magnitude, regardless of the intensity of the stimulus that generates the response. Muscle force is increased by either increasing the number of motor units that fire or by increasing the firing rate of the individual motor units. The amplitude measured is an instantaneous sum of all the action potentials generated at any given time. At any given pair of electrodes these action potential have both positive and negative components, which sometimes add and cancel rendering EMG a random-noise like waveform [8]. The characteristics of the EMG wave form depending on the type of electrode, the placement of the electrode, and the activity of the muscle is as follows:

Amplitude : 50 μ V to 5 mV.

Frequency: 10 Hz to 3000 Hz. [32].

Figure 1.12 shows a typical EMG signal obtained using surface electrodes from the biceps brachii.

1.5 Fatigue

Localized muscle fatigue is a term introduced by Chaffin[7]. According to his definition the condition is characterized by a progressive increase in discomfort arising from the active muscle as the prolonged constant force contractions at moderate to medium load levels are maintained. The subjectively felt discomfort is accompanied by specific changes in the EMG power spectrum (explained in section 1.6) of the muscle.

In the past, it was customary to think of muscle fatigue as the inability of a muscle to maintain either voluntarily or involuntarily a specified force output. This contractile fatiguability of muscles has been related to the muscle fiber types that comprise a muscle. Muscles with predominantly slow twitch motor units (type I) are more resistant to contractile fatigue than those that are more evenly mixed with slow and fast twitch motor units or a predominance of fast (type II) fibers [1]. By twitch is meant a brief contractile response of a skeletal muscle elicited by a single maximal volley of impulses in the motor neurons supplying it. Further this definition of fatigue is too subjective since it relies on the subject's desire to hold the contraction.

More recently, the concept of muscle fatigue has been considered as a continuous time dependent process throughout the entire contraction. Under this situation, the progression of fatigue has been associated with spectral shift of the EMG signal towards low frequencies.[12]. This shift in the power spectrum has been shown in Figure 1.13. Figure 1.13 A shows the spectrum of EMG before fatigue; Figure 1.13 B shows the shift in the spectrum (peak) of EMG towards low frequencies during fatigue.

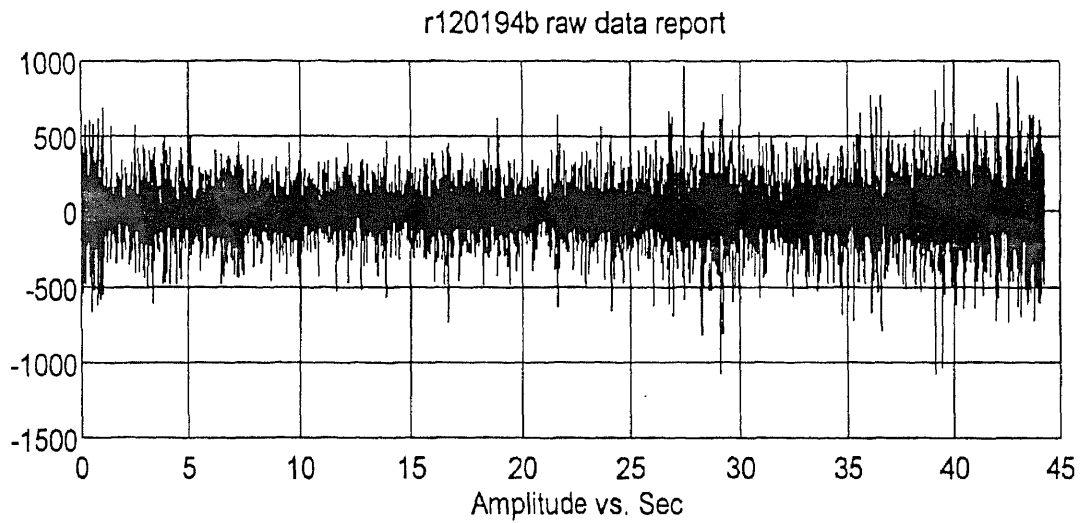


Figure 1.12 A typical EMG signal recorded from biceps brachii using surface electrode.

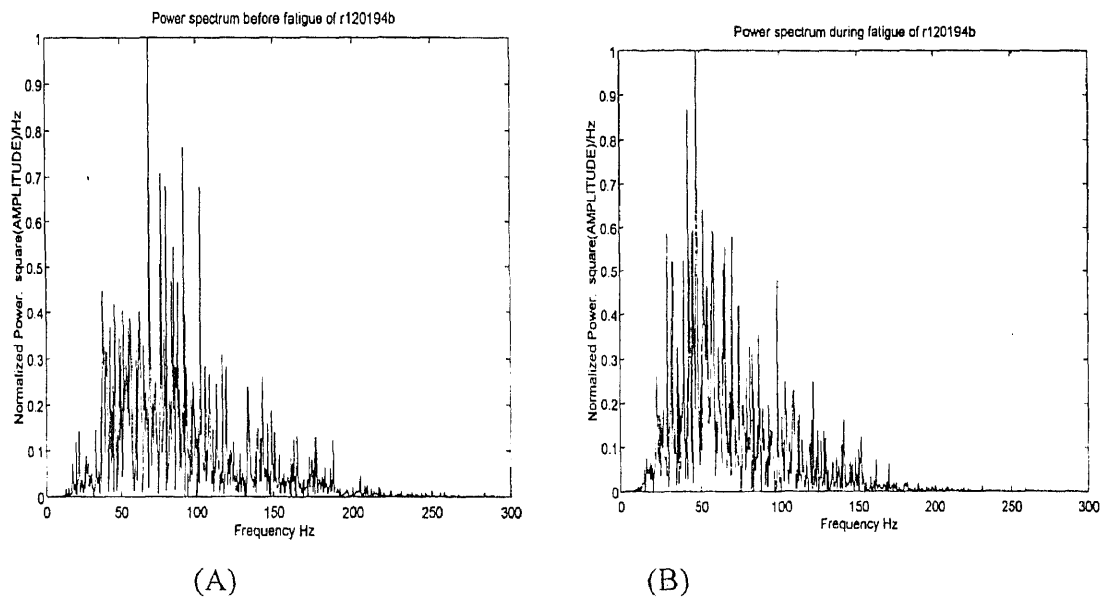


Figure 1.13 A shows spectrum of biceps brachii before fatigue; B shows spectrum during fatigue.

1.6 Mathematical Techniques

Use of digital computers for processing continuous or analog data involves digitizing, or the conversion to discrete values, of the data, as well as replacing the mathematical operations developed for the continuous data with operations for discrete data.

Sampling continuous data must be considered carefully, so that the digital data is a true picture of the continuous data. In order to avoid problems due to aliasing, the data must be sampled at a rate greater than twice the highest significant frequency found in the signal. This problem, as well as others pertaining to the use of data which are discrete and of finite length has been considered by various authors [2].

The processing formulation presented here is in discrete form to correspond to the digital processing. The sample mean of an individual sample function, computed by time averaging, is represented by

$$\bar{X} = \frac{1}{N} \left(\sum_{n=1}^{n=N} X_n \right) \quad (1.2)$$

where X_n are the data values and N is the number of data points.

\bar{X} is an unbiased estimate of the true mean value of the data points.

The EMG signal is a time and force dependent signal whose amplitude varies randomly above and below the zero. The data is transformed to zero mean to remove the dc level of the data. This is computed by

$$x_n = X_n - \bar{X} \quad (1.3)$$

where n goes from 1 to N .

After zero mean estimation, the data in the defined time window is subjected to fast Fourier transform (FFT). The Fourier transform is a signal representation that involve the

decomposition of the signals in terms of sinusoidal (or complex exponential) components. This kind of decomposition represents the frequency domain of the signal.

The FFT algorithm aids in the efficient computation of the discrete Fourier transform (DFT). Basically, the computational problem for the DFT is to compute a sequence $\{X(k)\}$ of N complex valued numbers given another sequence of data $\{x(n)\}$ of length N , according to the formula [39]

$$X(k) = \sum_{n=0}^{N-1} x(n) e^{-j2\pi kn/N} \quad 0 \leq k \leq N-1 \quad (1.4)$$

To simplify further, it is desirable to define the complex-valued phase factor W_N , which is the N th root of unity and is given by

$$W_N = e^{-j2\pi/N} \quad (1.5)$$

Therefore equation (1.4) becomes

$$X(k) = \sum_{n=0}^{N-1} x(n) W_N^{-kn} \quad 0 \leq k \leq N-1 \quad (1.6)$$

From equation (1.6) it is seen that for each value of k , direct computation of $X(k)$ involves N complex multiplications ($4N$ real multiplication) and $N-1$ complex additions ($4n-2$ real additions). Therefore, to compute all the values of a N point DFT requires N^2 complex multiplications and N^2-N complex additions. Considering this complexity, the FFT algorithm is used.

The FFT algorithm used is based on the number of data points in the time window. If the number of data points (N) is a power of 2, a radix-2 fast Fourier transform algorithm is used. Otherwise, a slow non-power-of-two algorithm is employed.[39].

The power spectral density function (PSDF) is then estimated by multiplying the data $X(k)$, where k goes from 1 to N , obtained as a result of the FFT, with its complex conjugate. This estimation is given by

$$P(f) = X(k) \times \text{conjugate}(X(k)) \quad (1.7)$$

This spectral estimation is the process of determining the spectrum of a signal, based on the actual measurement of the signal. The spectrum is a representation of the frequency content of the signal. This estimate gives the PSDF for the defined window size (N).

Considering the PSDF $P(f)$ as a weight function, the median frequency is computed by [45]

$$TP = \sum_{f=a}^{f=b} P(f). \quad (1.8)$$

$$\frac{\sum_{f=a}^{f_{med}} P(f)}{TP} = 1/2 \quad (1.9)$$

where TP is the total power, f is the frequency, f_{med} is the median frequency, P is the power spectral density at the frequency of interest ranging from low frequency (a) to high frequency (b). The median frequency is the frequency which divides the area under the spectral curve into two equal halves.

The mean frequency, that is, the average frequency is computed by

$$f_{mean} = \frac{\sum_{f=a}^{f=b} f \times P(f)}{\sum_{f=a}^{f=b} P(f)} \quad (1.10)$$

where a and b represent the bandwidth of the frequencies of interest [45].

Apart from performing frequency domain calculations from the zero mean data, the zero mean data is also subject to time domain parameters such as the root-mean-square (RMS) computation. The rms value is computed by [1]

$$RMS(x) = \sqrt{\frac{1}{N} \sum_{n=1}^{n=N} x^2} \quad (1.11)$$

These equations are organized in a flow chart as shown in Figure 1.14 demonstrating the computational part of the processing system.

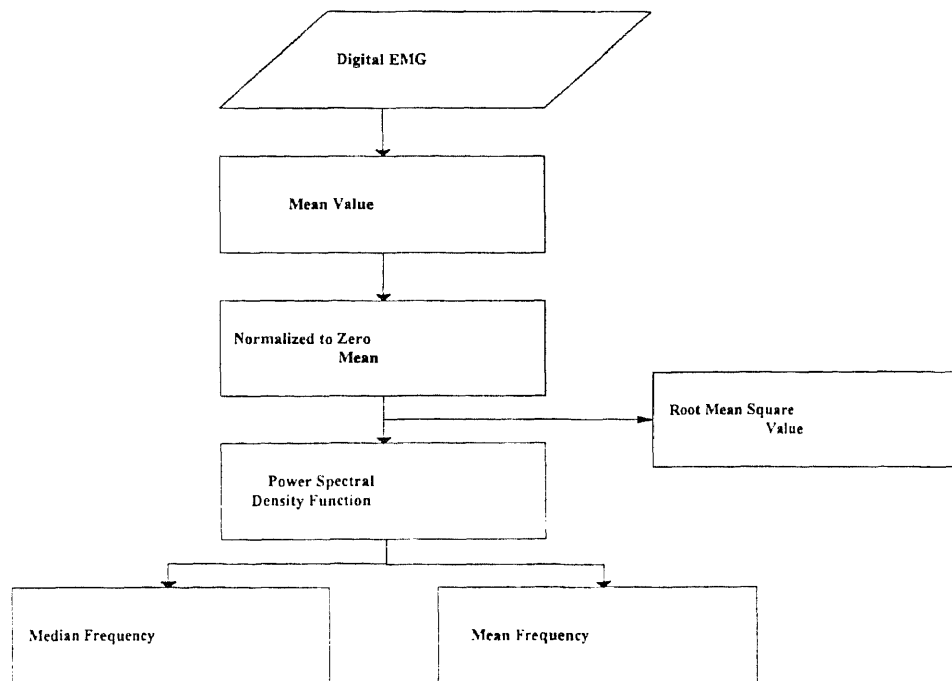


Figure 1.14 Computational parts of the processing system.

1.7 Statistical Techniques

The behavior of median frequency, mean frequency and RMS values of EMG with respect to time, determined using formulas 1.9, 1.10 and 1.11 can be best studied by performing linear regression analysis. Regression analysis is a statistical tool which utilizes the relation between two or more quantitative variable so that one variable can be predicted from the other, or others. [37]. The linear regression function can be given by

$$Y = A + BX \quad (1.12)$$

where X is the independent variable, Y is the dependent variable, A is the Y intercept of the regression line and B is the slope.

The regression parameters A and B are unknown and need to be estimated from the sample data. Once the data has been obtained the values of X and Y can be plotted. A good estimator of the regression parameters can be obtained by the method of least squares.

The principle of least squares estimation [23] involves minimizing the sum of the square deviations of the observed values from the mean, that is, it is required to find the value of the mean that makes the required sum as small as possible. The estimator slope

B is given by

$$Slope = \frac{Num}{Den} \quad (1.13)$$

where

$$Num = (\sum XY) - \frac{(\sum X \sum Y)}{n} \quad (1.14)$$

$$Den = \left(\sum X^2 \right) - \frac{(\sum X)^2}{n} \quad (1.15)$$

The Y intercept (A) is given by

$$Y \text{ intercept} = \frac{Up}{Den} \quad (1.16)$$

where

$$Up = \frac{(\sum X^2 \sum Y - \sum X \sum XY)}{n} \quad (1.17)$$

Den is equation (1.15) and n is the number of data points.

Thus with the data points, slope and y-intercept values, a regression line can be obtained. To estimated the degree to which the variables are related, correlation analysis can performed.

Correlation analysis gives only one number -an index that gives an immediate picture of how closely two variables move together. Correlation analysis and regression analysis are closely related mathematically and thus correlation becomes a useful aid in the regression analysis.

The coefficient of correlation **r** is given by

$$r = \frac{\sum XY - \frac{\sum X \sum Y}{n}}{\sqrt{\left[\left(\sum X^2 - \frac{(\sum X)^2}{n} \right) \left(\sum Y^2 - \frac{(\sum Y)^2}{n} \right) \right]}} \quad (1.18)$$

The value of r ranges from -1 to 1. A Positive value of the coefficient reflects the existence of a positive relationship, and a negative value reflects the presence of a negative relationship. The coefficient of correlation whose value is close to +1 or -1 indicates high degree of relationship between the variables, and the coefficient whose value is close to zero indicates a low degree of correlation [23].

Let us consider a plot which shows the behavior of the median frequency over time as the muscle fatigues. This plot is shown in figure 1.15.

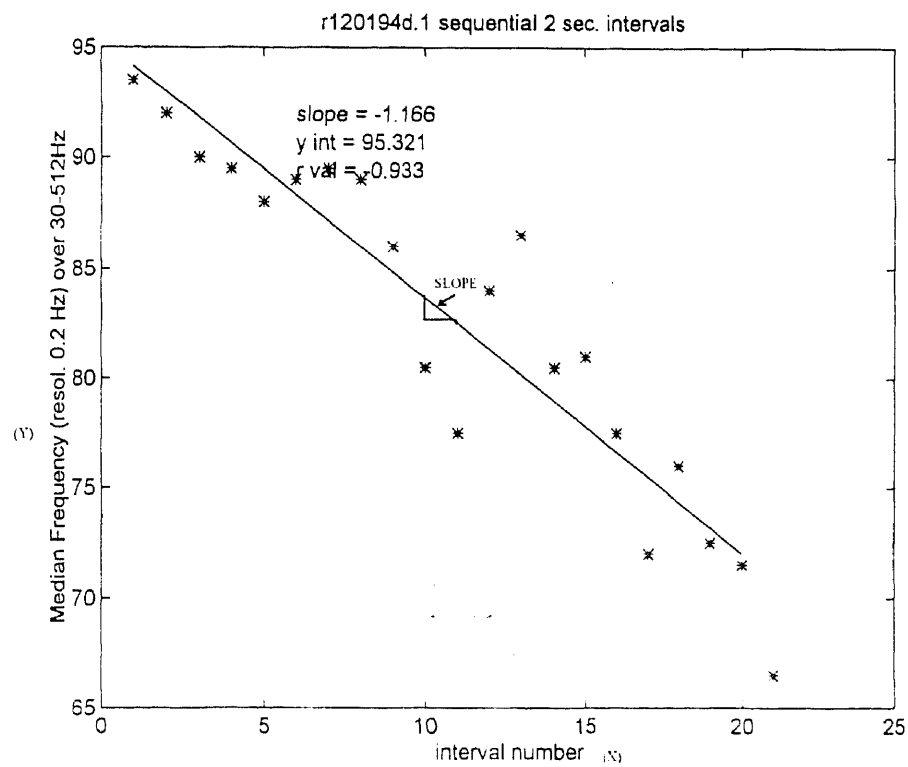


Figure 1.15 shows meaning of Linear regression parameters.

In the figure X is the time interval, Y is the median frequency, and assuming that n points (21 in the above figure) are available, then based on above calculations the linear regression fit would look as shown.. The figure also shows the slope, the y-intercept value and the correlation coefficient calculated using the above mentioned equations

1.8 Scope of the Thesis

The author was invited to participate in two ongoing research projects at the Kessler Institute for Rehabilitation on fatigue studies of muscles. The objective was to analyze the process of fatigue using signal processing techniques. These two project will be referred to as group I and group II.

1.8.1 Objective and Literature Review of Group I

The objective of this study was

1. To compare the frequency response of the Delsys™ and the Teca™ surface EMG electrode.
2. Determine the normal median frequency (MF) and the slope (index of fatigue) of MF decline with fatigue during isometric contractions of the upper extremity muscles, viz. biceps brachii, triceps and deltoid at 50% of maximal voluntary contraction (MVC) using spectral analysis of the surface EMG signal.

1.8.1.1 Hypothesis A normal value for median frequency and the slope of its decline during a fatiguing contraction exists for each muscle and has a small enough standard

deviation so that abnormalities, such as found in neuropathies and myopathies, can be differentiated from the normal values.

1.8.1.2 Significance Normal values of MF and MF decline with fatigue in specific muscles at a given level of isometric contraction have not been established. If normal values are determined for specific muscles, spectral analysis can be used clinically to evaluate patients with fatigue producing diseases such as chronic fatigue syndrome, multiple sclerosis, myopathies, neuropathies and motor neuron disease.

1.8.1.3 Physiologic significance of median frequency A decline in MF accompanies a sustained muscle contraction and has been correlated with muscle fatigue. MF begins to decrease early in a sustained contraction, prior to the subject's failure to maintain the required level of force, indicating metabolic fatigue of the muscle. The four possible explanations for the frequency shift:

1. changes in motor unit recruitment
2. changes in motor unit synchronization
3. change in muscle fiber conduction velocity
4. change in variability of motor unit discharge [1].

The frequencies in the low portion (0-40 HZ) of the power density spectrum reflect motor unit firing rate, but their impact on the MF is negligible because they represent only a small percentage of the total spectrum. Frequencies in the remainder of the spectrum are most affected by the shape of the motor unit impulse. Motor unit shape is

influenced by muscle fiber conduction velocity and tissue filtering properties. A decrease in conduction velocity produces a more dispersed waveform which will have more low frequency and fewer high frequency components. Human tissue acts as a low pass filter; as the tissue filtering effect increases, the low frequency content of the EMG signal will increase resulting in a lower MF [1].

Deluca [12], in his early experiment looked at the time dependent fatigue and frequency decay in the first dorsal interosseous (FID) and deltoid with sustained isometric contractions held until fatigue. The stronger the contraction, the more rapid the decline in frequency. The initial MF of the FID was greater than that of the deltoid, but their final values are similar.

Researchers have shown that frequency compression with fatigue is related to a decrease in conduction velocity (CV) along the muscle fiber [44]. However some researchers have shown that while the CV decline may contribute to MF decay with fatigue, supplementary factors must also contribute [6],[26],[34].

The median frequency has been shown to reflect the degree of motor unit recruitment [43]. This finding indicates that MF might be used as a tool to investigate recruitment strategies in different muscles. The median frequency is influenced by the type of contraction (static vs dynamic, ramp vs step), muscle pH, ischemia, cooling fiber type, immobilization, gender, and hand dominance. The most important factors pertaining to this study are the effects of fiber type, gender and hand dominance.

The type of fiber has a tremendous effect both on initial MF and MF decay with fatigue. Fiber type accounts for most of the differences in power density spectra of

various muscles. Researchers have shown that the magnitude of frequency shift with fatigue is dependent on the percentage of type II fibers with type I fibers being more fatigue resistant [12] ,[31]. Many studies of MF behavior have not taken gender into account. Bilodeau [3] showed that the change in MF during 5 second ramp contractions of the biceps and triceps from 0-100% MVC follows a different pattern in males and females. A recent study showed that gender had a significant effect on the slope of MF decay with fatigue in biceps (-0.98 for males vs -0.64 for female) [29]. Dominance also appears to influence the MF of a muscle. Deluca [12] compared initial MF in the left and right first dorsal interosseus of both right and left hand subjects. It was noticed that in males the MF was higher in the non-dominant hand of right handed subjects and no left-right differences were detected in left handed males. No right-left differences were detected in the female subjects, but initial MF was higher in females than males. These results have been interpreted as suggesting that the dominant, more used muscle develops more twitch fibers resulting in a lower initial MF.

The measurement of MF using surface electrodes has been shown to have excellent intra-subject reliability but a large degree of variability between individuals. Deluca [12] found a coefficient of variability of only 2.4% when subjects repeated contractions of the FDI on 3 consecutive days at 4 different force levels. Dannen [9] had five subjects perform isometric contractions of the biceps on 5 consecutive days. The MF varied from 65 - 95 Hz for the five subjects with a standard deviation of 11.5 Hz. However, the standard deviation for trials within each subject was 2 Hz.

1.8.2 Objective and Literature Review of Group II

1. The objective of this group was To determine whether single fine wire as an active electrode referenced to a surface electrode (monopolar fine wire) can validly and reliably measure muscle fatigue by the fatigue indicators median frequency (MF), mean frequency (MNF) and root-mean-square (RMS).
2. To determine if monopolar fine wire is equivalent to or better than a bipolar surface electrode for measuring MF, MNF, and RMS.
3. To determine what distance between two bipolar fine wires consistently and reliably detects MF, MNF, and RMS.

1.8.2.1 Null Hypothesis

1. No differences exist between the use of bipolar surface, bipolar fine wire, and monopolar fine wire electrodes for the detection of MF, MNF and RMS.
2. No difference in muscle fatigue measurement exists between bipolar fine wire electrodes placed apart by a distance of one, two, or three centimeters.
3. No difference exists between bipolar fine wire electrode and monopolar fine wire electrodes for MF, MNF, and RMS.

The characteristics of the EMG signal changes as the muscle remains in a contracted state for an extended period of time, indicating muscle fatigue. As the muscle begins to fatigue, there is a change in the median frequency (MF), the mean frequency

(MNF) , the root-mean-square (RMS) of the EMG signal, and the conduction velocity (CV) in the muscle fiber. [1],[6],[35].

As muscle fatigues there is a decline in MF and MNF [12],[14],[47] and an increase in the RMS of the EMG signal [26],[27]. Most of the EMG studies have been performed using surface electrodes [41]. Recently attention has turned towards the use of intramuscular (fine wire) electrodes to measure the signal more directly, and to avoid the impedance of the tissue overlying the muscle under study [44].

Further, fine wire electrodes also have the advantage of being able to detect deeper muscle structures, and avoid the interfering signals from more superficial muscles. Stashuk and Deluca [44] compared a 0.45 mm intramuscular cannula to monopolar and bipolar surface electrodes to determine the MF of muscles contracting at 80% MVC. They found that the surface bipolar signals had faster rates of decline and some had higher values of MF when compared to both monopolar surface and cannula signals. Cannula and monopolar surface signals had similar initial MF, but the monopolar surface signal displayed greater rates of decline. Their conclusion was that spatial filtering and intermuscular tissue impedance were responsible for the differences in spectral shifts between the surface and indwelling methods of detection. The study does not clearly explain how the cannula electrode signals were referenced, nor do they provide explanation concerning their conclusions. In contrast, a previous study at the Kessler Institute for Rehabilitation using hand-held weights until fatigue [11] showed bipolar surface and bipolar fine wire signals to have similar initial MF, with greater MF decline

observed in the fine wire signal. A thorough search in the literature on this subject indicated that no similar study of this kind had ever been reported.

1.9 Body Fat Estimation

This section describes the procedure, used in both the projects, to estimate total body fat in subjects. The purpose of fat estimation was different in both projects. For group I fat measurement was made to find out if %body fat had any influence on establishing normal median frequency values. For group II, it was necessary to estimate body fat in order to standardize the depth of insertion of the fine wire electrode to ensure that the wire is in contact with muscle fiber and not on fat.

The assessment of total body fat can be made indirectly by the measurement of skinfold thickness [16]. The procedure involves measuring skinfold on the subscapular and thigh using a skin fold caliper (Cambridge Scientific Industries- Lange). These positions are shown in figure 1.16.

These two values are used to determine the body density using the formula [42]

$$\text{Body Density} = 1.1043 - (.00131 \times \text{subscapular}) - (.001327 \times \text{thigh}) \text{ gm/ml.} \quad (1.19)$$

From the body density, total body fat can be determined using the formula [18]

$$\text{Body fat present} = (4.57/\text{Body density} - 4.142) \times 100 \quad \% \text{ Body Fat} \quad (1.20)$$

The value of body fat estimated by the above procedure is then compared to the classification table [18] to determine the category to which the subject belongs.

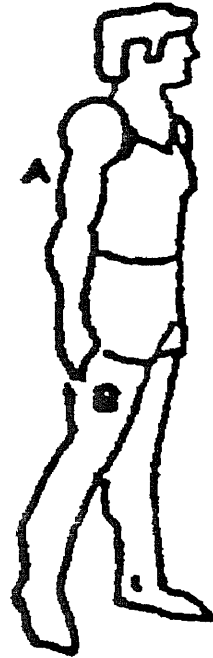


Figure 1.16 Location of skin fold measurements in male subjects. A : Subscapular; B: Thigh.

Table 1.1 Body fat norms

CLASSIFICATION	MEN (%)
Very low fat: skinny	7.0 - 9.0
Low fat: trim	10.0 - 12.9
Average fat: normal	13.0 - 16.9
Above normal fat: plump	17.0 - 19.9
Very high fat: fat	20.0 - 24.9
Obese: over fat	25.0 and higher

CHAPTER 2

METHODS

This chapter describes the experimental setup, procedure for acquiring data and signal processing tools used for the analysis of the time and the frequency components of the EMG signal for the two ongoing research projects at the Kessler Institute for Rehabilitation.

The first project concerns comparing the frequency response of the Delsys™ and the Teca™ surface electrodes and determining the normal values for the median frequency in upper extremity muscles during isometric contraction at 50% of maximum voluntary contraction using the Delsys electrode. This project will be referred to as group I. The second project concerns developing a new technique for measuring muscle fatigue using monopolar and bipolar fine wire electrodes. This group will be referred to as group II.

2.1 Experimental Setup for Group I

In the first part of this study, two types of surface electrodes were compared. In each volunteer, three muscles in the upper extremity were tested with both the electrodes placed on the muscle under study. These muscles were biceps, triceps and deltoid. All these muscles were tested with the subject supine on a plinth with torso stabilized by a therapist. In the second part, in each volunteer, the same three muscles in the right upper extremity were tested in a circuit fashion using the Delsys electrode. By circuit

fashion is meant testing all the remaining muscles before retesting a muscle. All the upper extremity muscles were tested with the subject supine on a plinth with torso stabilized by a therapist.

2.1.1 Electrode Placement and Mounting

For the first part for the study, after the skin of the subject was cleaned, prepped with OMNI-PREP™ and allowed to dry, a bipolar Teca™ (#922-6030-1) surface EMG electrode with gel on its active electrode was placed on the insertion site of the muscle under study as discussed in chapter 1. The reference electrode was placed distal to the active electrode with the midline of the muscle belly in the direction of the muscle fibers. A pasteless bipolar surface EMG differential Delsys™ (#DE02) electrode was placed in parallel and as close as possible to the Teca electrode. Both electrodes were attached to the skin with cloth tape (Kendall-Curasilk). A saline-soaked strap located at the wrist provided a ground reference.

For the second part of the study, a pasteless bipolar surface EMG differential electrode (Delsys #DE02) was placed with its active electrode on the insertion site of the muscle under study as discussed in chapter 1. The reference electrode was placed distal to the active electrode along the midline of the muscle belly in the direction of the muscle fibers. This recording electrode was attached to the skin with cloth tape (Kendall-Curasilk). The contacting surfaces of the electrode were depressed 1-2 mm relative to the surrounding skin, due to elasticity of the cloth tape. The subcutaneous soft layer was slightly compressed to raise the EMG amplitude and to obtain better signal to noise ratio.

This dry or pasteless electrode does not require any skin preparation or paste. However, the skin was cleaned with alcohol swabs and was allowed to dry to make it free of dirt and oil. A saline-soaked strap located at the wrist provided a ground reference.

2.1.2 Testing Protocol

For the first part of the study the subject was required to perform 3 maximum isometric contractions for each muscle under study. This contraction was performed against a manual resistance offered by the tester using a hand held dynamometer (Sensotech's precision miniature load cell #31 and signal conditioning display instrument GM unit). The greatest value of the three trials was used as the subjects maximal voluntary contraction (MVC). Once the MVC was found, the subject was tested at 50% of the MVC for a 45 second period for all the muscles.

For the second part of the study the subject was required to perform 3 maximum isometric contractions for each muscle under study. This contraction was performed against a manual resistance offered by the tester using a hand held dynamometer (Sensotech's precision miniature load cell #31 and signal conditioning display instrument GM unit). The greatest value of the three trials was used as the subjects maximal voluntary contraction (MVC). Once the MVC was found, the subject was tested at 50% of the MVC for a 45 second period. Three such trials were performed for each muscle in a circuit fashion with 10 minutes rest period between successive trials. It has been shown that the median frequency recovers essentially five minutes after the contraction is finished [12]. The subject's %body fat was determined as discussed in section 1.9

2.2 Experimental Setup for Group II

In this study the muscle of interest was the biceps brachii. Both fine wire and surface electrodes were used to record the EMG signal of the biceps brachii during contraction.

2.2.1 Electrode Placement and Mounting

First, the distance between the humeral epicondyles of the nondominant arm was measured using a set of calipers. The elbow was then flexed and maintained at 90 degrees using a Goniometer. A line bisecting the upper and lower arm was drawn.

With the elbow maintained in a flexed position, the distance between the acromioclavicular (AC) joint and midpoint of the antecubital fossa (ACF) was determined. Three fourth the distance between the AC and the ACF was determined and marked along the bisecting line of the distal upper arm. Point FW2 was marked one centimeter distal to the intersection of these two lines. Point FW1 was marked at the intersecting lines and point FW3 was marked exactly one centimeter below the point FW2 along the bisecting line.

After determining these positions, 20 μm diameter teflon coated stainless steel composite fine wires with 2 mm of exposed end were inserted into the points FW1, FW2, FW3 at a depth of 15-20 mm using a 27 gauge cannulated needle. This needle can be withdrawn easily and its removal only rarely dislodges the electrode as they are retained by the hooks at their ends. The electrodes were taped to the skin at the site of emergence to ensure that an accidental tug does not remove them.

Immediately next to the fine wire, the skin was cleaned , prepped with OMNI-PREP™ and was allowed to dry. A bipolar bar electrode (Teca #922-6030-1) with gel on its active and reference electrode was attached with cloth tape(Kendall-Curasilk), with the active electrode close to the point FW1 and the reference electrode placed distally along the bisection line in the direction of the muscle fiber. Electrode placement on the distal upper arm is shown in figure 2.1.

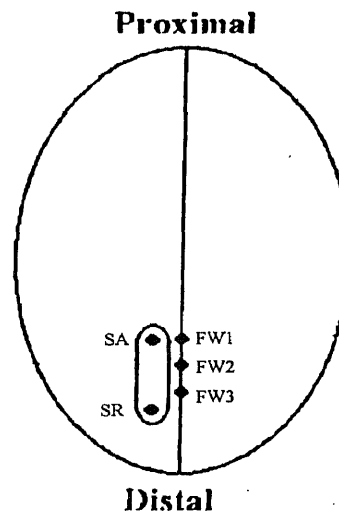


Figure 2.1 Electrode placement on the distal upper arm. SA and SB are surface bipolar electrodes; FW1, FW2 and FW3 are fine wire electrodes.

The bipolar electrode used was cleaned before each application to remove any residual gel by wiping with gauze dampened in distilled water. The dead surface layer of the skin along with the protective hair was removed to lower the electrical impedance by light abrasion of the skin at the site of electrode placement. The gel acts at the skin-electrode interface by offering good electrical contact.

A silver disc surface electrode with gel, attached with tape at the wrist, acted as a ground reference. The skin beneath the ground electrode was also prepared and cleaned.

2.2.2 Testing Protocol

In order to determine 15% of the subjects lean body weight, the subject, with no neuromuscular disease, was weighed in light clothing at the beginning of the experiment, using a 500 pound maximum Toledo precision weight scale. Next the Subjects % body fat was determined as described in section 1.9. Then surface and fine wire electrodes were placed as described in section 2.2.1.

The subject was then asked to maintain the arm at 90 degrees flexion and hold a dumbbell, weighing 15% of the subject's lean body weight, for 30 seconds. The EMG recording from 8 channels formed as result of different combinations of monopolar and bipolar electrodes were made as shown in table 2.1. After the subject rested for 30 minutes, the second trial was performed in a similar fashion as the first trial. The subject was retested after one to two weeks following the same protocol.

2.3 Data Acquisition for Group I

For the first part of the study the EMG signal available at the surface of the skin was picked up by both Teca and the Delsys electrodes. The Delsys electrode has built-in circuitry that amplifies the signal 10 times. The EMG signal for both electrodes was fed to an isolated preamplifier (Gould #11-5407-58). This preamplifier in turn was connected to a signal conditioner universal amplifier (Gould #13-4615-58). In the amplifier the

signal was bandpass filtered between 30 Hz and 1000 Hz and was amplified 200-600 times (varied from subject to subject). It was always ensured that the gain of the amplifier to which the Teca electrode was connected was 10 times higher than the Delsys, which amplifies the signal 10 times before sending it to the amplifier, in order to make the gain equal on both the channels for accurate comparison.

Table 2.1 Electrode configuration used for Group II

ELECTRODE	CHANNELS							
	1	2	3	4	5	6	7	8
Surface Active (SA)	*				*ref			
Surface Reference (SR)	*ref					*ref	*ref	
Fine Wire 1 (FW1)		*		*	*	*		*ref
Fine Wire 2 (FW2)		*ref	*					
Fine Wire 3 (FW3)			*ref	*ref			*	*
Subject Ground	•	•	•	•	•	•	•	•

* refers to active electrode; *ref refers to reference electrode; • refers to ground electrode

This universal amplifier is housed in a Gould 5900 cage. The conditioned analog data were fed into a 12 bit resolution analog to digital interface board (Kiethley MetraByte #DAS1601) through a screw terminal accessory board (Kiethley MetraByte

#STA-16). This converted digital data were stored in binary form on an IBM compatible 286 PC using data acquisition software (Kiethley MetraByte #STREAMER v3.25). The output of the signal conditioner unit was monitored on a 4 channel digitizing oscilloscope (TekTronix #TDS 455A) during muscle contraction to ensure absence of noise, 60 Hz interference or motion artifacts.

For the second part of the study the EMG signal available at the surface the skin was picked up only by the Delsys electrode. The other stages of the acquisition were the same as the first part. In addition to acquisition of the EMG signal, the force output from the hand held dynamometer was also fed to one channel of the A/D board and was recorded for a 45 second duration. The instrumentation details are in Appendix B and the protocol for the data acquisition is in Appendix C.

2.4 Data Acquisition for Group II

The EMG signal from 8 different electrode configurations discussed earlier, was fed to an isolated preamplifier (Gould #11-5407-58). This preamplifier in turn was connected to signal conditioning universal amplifier (Gould #13-4615-58). In the amplifier the signal was bandpass filtered between 30 Hz and 1000 Hz and amplified 200-600 times (varied from subject to subject). Eight such universal amplifiers are housed in a Gould 5900 card cage. The conditioned 8 channel analog data were fed into a 12 bit resolution analog to digital converter interface board (Kiethley MetraByte #DAS1601) through a screw terminal accessory kit (Kiethley MetraByte #STA-16). The converted data were then stored in binary form in an IBM compatible 286 computer using data acquisition software

(Kiethley MetraByte # STREAMER V3.5). The output of the signal conditioner units were monitored using a 4 channel digitizing oscilloscope (Tektronix #TDS 455A) during muscle contraction to check for signal free of any noise or artifact.

2.5 Data Analysis for Group I

For both the parts of the study data analysis was performed off-line. The data were sampled at 2000 samples per second which limited the spectral frequency range to 1000 Hz. However, in this study the PSDF was defined in the range of 30 Hz -512 Hz because no useful information was found beyond 512 Hz and it has been pointed out [kwan] that below 30 Hz there exists low-frequency noise due to polarization potentials and motion-induced potentials between the skin and electrode that render very low frequency observations useless.

For the first part of the study the entire 45 seconds of the EMG signal from both the electrodes stored in binary form was imported to an IBM compatible 486 computer for fast digital signal processing. The data stored in binary mode were converted to ascii using special software (Kiethley MetraByte #STREAMER v3.5 - UNPACK utility). This unpack utility places a comma (,) as the delimiter between the data points and also places channel numbers in the first row of the converted ascii file. The ascii data file with comma as delimiter between the data is not in a form compatible with MATLAB™ v4.2b (The Math works Inc.). Hence the unpack code, written in C language, was modified to make the converted ascii file free of channel numbers in the first row of the file and to

remove the comma after each data. This modified code is named KUNPACK2.

MATLAB was the signal processing software used for the analysis.

The 45 sec file was divided into blocks of 2 sec of data. The first block of data was rejected to compensate for delay and any muscle movement artifact often observed during the first second of contraction, and for each of the remaining 21 block of the 2 channels of the raw data, the sample mean was computed in order to remove the DC level from the data. Next the FFT was applied on the transformed data to obtain the PSDF. From the resulting PSDF the median frequency was computed as described in the previous chapter. This resulted in 21 median frequency points for each channel were passed into a program developed to perform linear regression by the method of linear least squares. The slope (the fatigue index), y-intercept (the initial median frequency) and correlation coefficient were obtained for the fit. The output of the plot was studied to observe the changes in median frequency over the 45 sec contraction. The y intercept, which reflects the initial median frequency, that is, frequency just at the beginning of the contraction, and the slope, which indicates the amount of fatigue, were then used to understand the nature of fatigue and the correlation coefficient value was used to see how the median frequency points are related to one another. However, the most important parameter of interest was the initial median frequency value (y intercept) as it reflects since we wanted to compare the frequency response of both electrodes tested at the same time and under the same test conditions.

All algorithms were coded in Matlab Language. The program requested the name of the file to be analyzed and the size of the block for analysis and produced 2 plots.

1. Raw EMG data report for both the channels.
2. Median frequency plot for both the channels with slope, y-intercept and correlation coefficient values.

The analysis in the second part of the study was the same as for the first part except that the data processed were the EMG signal picked up by the Delsys electrode and the force output from the transducer. All algorithms for analysis were coded in Matlab language. The program requested the name of the file to be analyzed and the size of the block for analysis and produced 3 plots.

1. Raw EMG data report.
2. Raw force report.
3. Median frequency plot with slope, y-intercept and correlation coefficient values.

See Appendix D for flow chart and programming details.

2.6. Data Analysis for Group II

Data analysis was performed off-line. In this study the data were sampled at 3000 samples per second which limited the spectral frequency range to 1500 Hz. The high sampling rate was chosen for this study as it was assumed that the fine wire EMG signal can contain frequencies as high as 1000 Hz. In this study the PSDF was defined in the range of 30 Hz-1000 Hz. The sampling rate chosen is well within the limit defined in the sampling theorem, which states that the sampling rate must be at least twice the highest frequency found in the signal.

The entire 30 seconds of 8 channel EMG signal stored in binary form was transferred to an IBM compatible 486 PC for fast processing. The data stored in binary form was converted to ascii form as described in section 2.5.

Due to limitations in the unpack utility for handling large samples of data and large memory requirement in MATLAB a batch program was developed to divide the 30 seconds of 8 channel EMG signal into 15 files of 2 seconds each. Each of the 2 second files contained 8 channels of data.

This study involved comparing the median frequency, mean frequency and root mean square value of the EMG between surface and fine wire electrodes. A program was developed in MATLAB language which loaded 2 second files one after the other. The first 2 seconds of data was rejected to compensate for any delay. Each loaded 2 second file was first processed channel by channel to compute the sample mean and the data were then transformed to zero mean for reasons described in the previous section. The fast Fourier transform was applied on the transformed data to obtain the PSDF. From this resulting PSDF, mean frequency and median frequency were computed as described in the previous chapter. The raw EMG data was sent to a subprogram developed to calculate the root mean square value (RMS) to observe EMG changes in the time domain.

Similarly, the remaining sections were processed to obtain 14 median frequencies, 14 mean frequencies and 14 rms points for each channel. These 14 points of frequency domain and time domain signals were passed into a program developed to perform linear regression by the method of least squares. The slope (the fatigue index), y-intercept (the initial frequency/rms) and correlation coefficient were obtained for the fit. The output of

the plot was studied to see how these time domain and frequency domain parameters behave over 30 sec contraction for each of the channels.

Programs were required for creating fifteen 2 second files and for signal processing. The first program asked for the name of the binary file and converted a 30 sec file to 15 ascii files of 2 seconds each. The other program requested the name of the file, the size of the block for analysis and total duration of the experiment and produced 32 plots as follows:

1. 8 raw EMG data reports.
2. 8 root mean square plots.
3. 8 median frequency plots.
4. 8 mean frequency plots.

Figure 2.2 shows the block diagram of the instrumentation system common to both the projects.

See Appendix D for the flow chart and programming details.

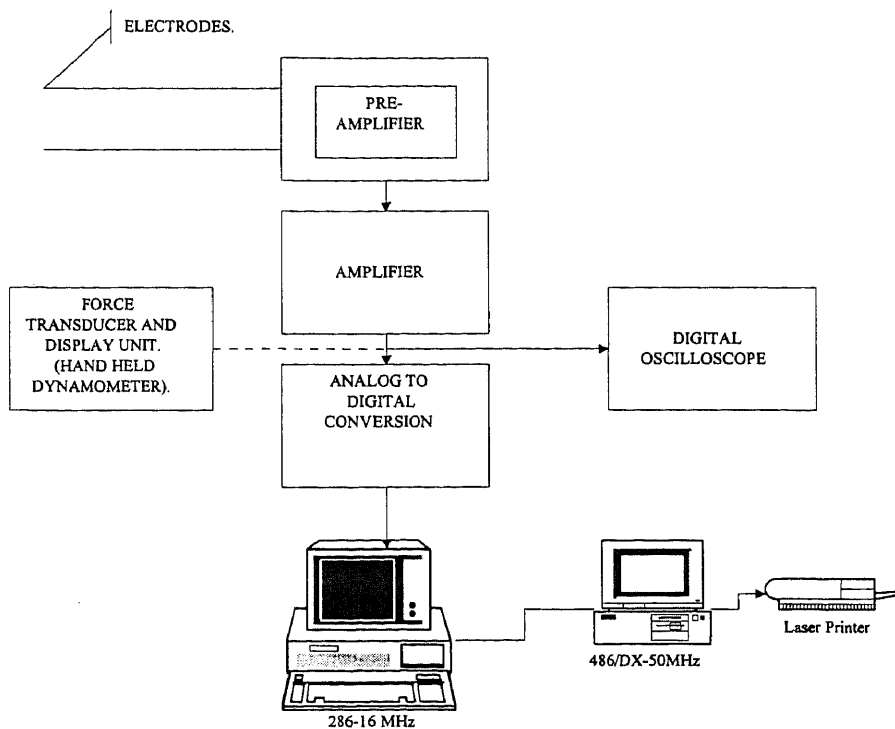


Figure 2.2 Block diagram of instrumentation system common to both the projects except for the force transducer which was used only for group I

CHAPTER 3

RESULTS

This chapter details the result of the pilot study of the two ongoing research projects as described in chapter 2. The experiments for both projects were performed as per the protocol described in the previous chapter and the results obtained were as follows:

3.1 Results of Group I

In this section, before discussing the experimental results, we will discuss the part of the study concerning the comparison of two different kinds of surface electrodes.

3.1.1 Comparison of Delsys™ and Teca™ Surface EMG Electrode:

The objective of this group was to find the normal median frequency in the upper extremity muscles during isometric contraction at 50% MVC using surface EMG. It has been widely reported that a higher initial median frequency (IMF), (the value at the beginning of a sustained contraction) value was obtained using the Delsys electrode [6] . The high initial median frequency is important because it shows wide frequency response of the Delsys therefore, more information about the EMG is being picked up. Further, this parameter is clinically important as reported in previous studies [30] that their exists difference in the IMF between the normals and the patients with neuromuscular disease such as myopathies and neuropathies. It has also been reported that myopathy subjects have shown high IMF compared to the normals and those with neuropathy have show

less IMF. Hence this parameter becomes very important for the second part of this study concerning finding the range of IMF for the different muscles. Therefore the investigators wanted to compare the Delsys electrode with the Teca electrode, which was used in previous studies [11].

After preparing the skin, as explained in the section 2.1.1, both electrodes were placed adjacent to one another over the upper extremity muscles, the biceps, triceps and deltoid. The muscles were tested as described in chapter 2 for a 30 sec duration. The EMG signal obtained simultaneously from both electrodes were processed for median frequency and subsequent linear regression and correlation analysis. The y-intercept (the initial median frequency) , slope (the fatigue index) and the correlation coefficient for all experiments were computed. Since the parameter of interest was the initial median frequency, its value obtained from several trials is shown in table 3.1.

Table 3.1 Delsys™ Vs Teca™ with regards to initial median frequency

Trial #	Biceps		Triceps		Deltoid	
	Y intercept (Hz)		Y intercept (Hz)		Y intercept (Hz)	
	Delsys™	Teca™	Delsys™	Teca™	Delsys™	Teca™
1	68	54	109	86	74	79
2	92	81	91	83	98	103
3	126	78	61	51	112	67
4	125	51	94	79	104	98
5	109	76	91	83	78	70

It is observed from the table that the initial median frequency (y-intercept) value, except for a few cases, is higher for the Delsys electrode than for the Teca electrode. F Figure 3.1 shows the comparison of both the electrodes with ch1 representing the Delsys

electrode and ch2 representing the Teca electrode. Therefore, because of these result, the Delsys was used for the remainder of the study.

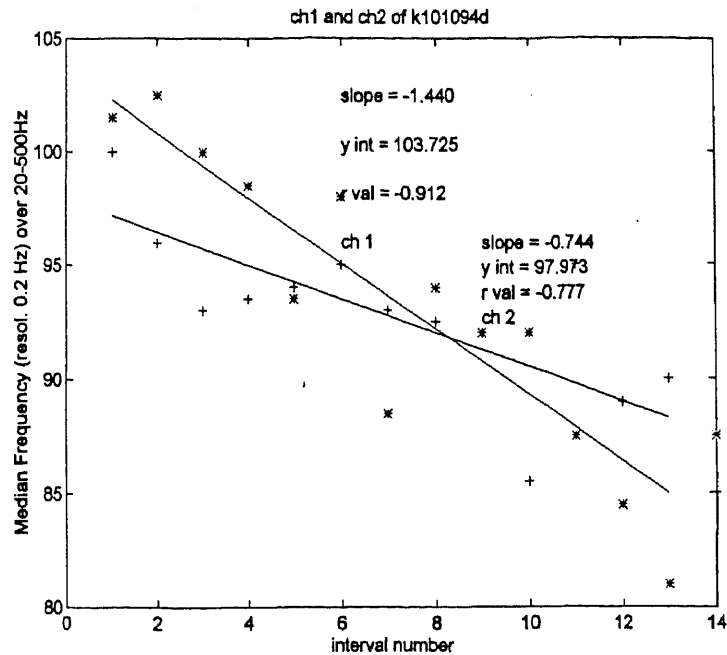


Figure 3.1 shows the comparison of the Delsys (ch1) with the Teca (ch2) surface EMG electrode of trial 4 on deltoid muscle.

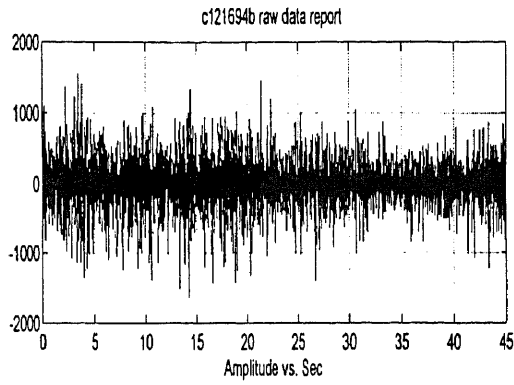
3.1.2 Experimental Results

A pilot study on the manual testing of the upper extremity muscles, the biceps, triceps and deltoid, was performed in circuit fashion 3 times as described in section 2.1 on 6 male volunteers (mean age, 25 (standard deviation (SD) 3) years; mean height, 70 (SD 3) inches; mean weight, 159.7 (SD 20.3) lbs; mean body fat, 17 (3.5 SD) %). The slope, y intercept and correlation coefficient values obtained as a result of applying a linear fit to the median frequency points obtained from each trial has been tabulated in table 3.2.

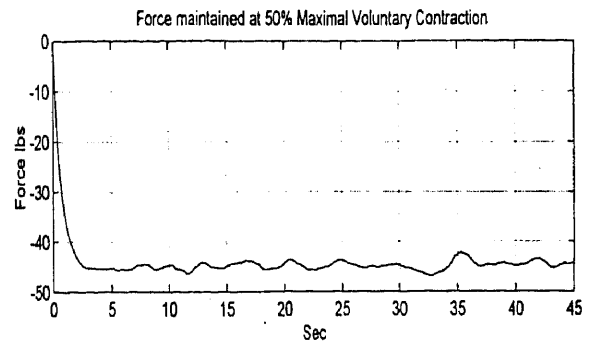
Figure 3.A shows plot of raw EMG and B shows the force level maintained at 50% MVC during that trial. Figure 3.3 shows one trial with a correlation coefficient -0.890.

Table 3.2 shows the linear regression and correlation parameters of the 3 muscles.(values followed by asterisk (*) were not used for the mean computations).

SUBJECT	MUSCLE	TRIAL #	SLOPE	Y intercept	CORR. COEFF	Mean	
						Slope	Y int
1	Biceps	I	-0.512	66.017	-0.779	-0.55	68.1
		II	-0.488	62.983	-0.729		
		III	-0.656	75.817	-0.721		
	Triceps	I	-4.184	165.093	-0.857*	-0.43	79.2
		II	-0.423	76.110	-0.582		
		III	-0.418	82.219	-0.559		
	Deltoid	I	-2.292	119.857	-0.973	-1.65	111.9
		II	***	***	***		
		III	-1.008	103.951	-0.808		
2	Biceps	I	-0.413	126.567	-0.281*	-0.94	119.2
		II	-0.581	131.012	-0.378*		
		III	-0.944	119.171	-0.599		
	Triceps	I	-0.441	88.993	-0.617	-0.57	88.1
		II	-0.701	87.183	-0.763		
		III	0.034	83.312	0.062*		
	Deltoid	I	-0.647	99.686	-0.751	-1.17	101.2
		II	-2.024	115.717	-0.970		
		III	-0.827	88.188	-0.739		
3	Biceps	I	-1.199	109.376	-0.927	-1.13	111.2
		II	-1.188	107.643	-0.901		
		III	-1.005	116.431	-0.882		
	Triceps	I	-0.533	88.388	-0.713	-0.39	88.5
		II	-0.240	86.993	-0.505		
		III	-0.407	90.098	-0.560		
	Deltoid	I	-0.240	82.398	-0.401*	-0.6	92.9
		II	-0.631	92.460	-0.764		
		III	-0.568	93.338	-0.776		
4	Biceps	I	-0.277	85.217	-0.545	-0.69	93.7
		II	-1.103	102.176	-0.836		
		III	-0.379	87.998	-0.468*		
	Triceps	I	-0.434	69.890	-0.803	-0.41	74.8
		II	-0.383	77.095	-0.633		
		III	-0.406	77.464	-0.739		
	Deltoid	I	-0.695	88.960	-0.890	-0.99	93.0
		II	-1.184	95.926	-0.90		
		III	-1.103	94.231	-0.907		
5	Biceps	I	-0.648	106.605	-0.683	-1.35	116.8
		II	-1.503	120.290	-0.890		
		III	-1.906	123.590	-0.905		
	Triceps	I	-0.534	93.593	-0.741	-1.07	94.9
		II	-1.434	100.557	-0.946		
		III	-1.227	90.571	-0.921		
	Deltoid	I	-0.615	77.764	-0.869	-0.61	76.9
		II	-0.772	76.993	-0.934		
		III	-0.432	75.995	-0.779		
6	Biceps	I	-0.185	85.250	-0.340*	reject	reject
		II	0.242	85.590	0.411*		
		III	-0.353	90.379	-0.494*		
	Triceps	I	-0.270	81.495	-0.457*	-0.8	82.0
		II	-0.814	75.814	-0.863		
		III	-0.784	88.264	-0.839		
	Deltoid	I	-0.129	95.350	-0.172*	-0.86	108.0
		II	-0.788	105.957	-0.791		
		III	-0.931	110.117	-0.866		



(A)



(B)

Figure 3.2 (A) shows EMG and (B) shows the force level maintained at 50% MVC by subject 5, trial 2, triceps

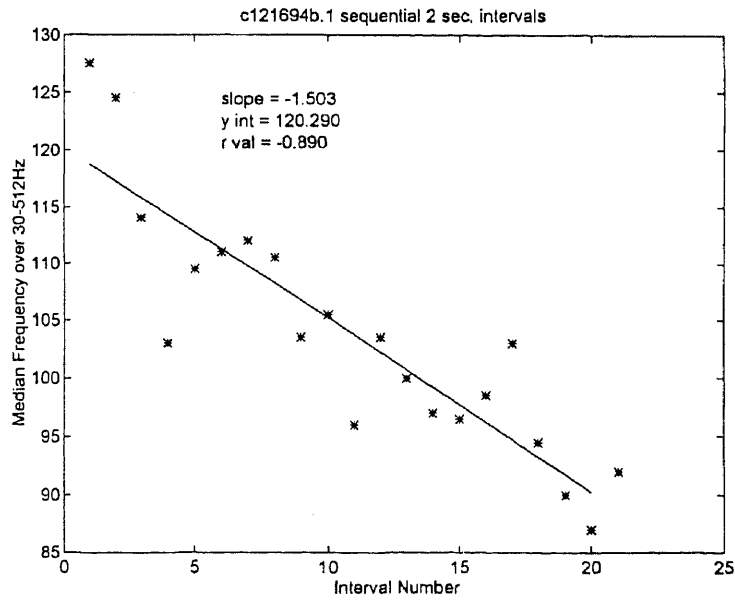


Figure 3.3 shows least squares fit to median frequency data: good fit subject 5, biceps, trial 2.

The mean value of the 3 trials of each muscle was computed for all the volunteers. The trials with correlation coefficient less than 0.5 were rejected. The normal range of values of median frequency and slope based on mean initial median frequency value and mean slopes of 6 subjects for the three muscles were computed and the result is shown in table 3.3 with 95% confidence interval.

Table 3.3 shows the range of normal median frequency values of 3 muscles.

Muscle	Mean Y int	SD	With 95% confidence level (mean \pm 2SD) (Hz)	mean slope	SD	with 95% confidence level (mean \pm 2SD)
Biceps	101.8	21.3	59.2 to 144.4	-0.932	-0.32	-1.6 to -0.3
Triceps	85.0	6.5	72.0 to 98.0	-0.61	0.27	-1.2 to -0.07
Deltoid	97.3	12.6	72.1 to 122.5	-0.98	0.4	-1.78 to -0.18

SD refers to standard deviation

The results showed a wide range for the median frequency of the biceps muscles (59.2 to 144.4 Hz). We believe that such a wide range of the median frequency for this muscle may be because the test was performed on only 6 subjects which gave us a high standard deviation of 21.3. However, we believe that by completing this study on 62 subjects we will see a smaller range.

A non parametric analysis of variance was performed to check for any significant differences in the initial median frequency and the fatigue index of the 3 muscles. A p value of 0.164 (Kruskal-Wallis test) for the initial median frequency and 0.106 for the slope was obtained based on the data available from the 6 volunteers. This analysis showed no significant differences in the initial median frequency and slope among the three muscles.

3.2 Results of Group II

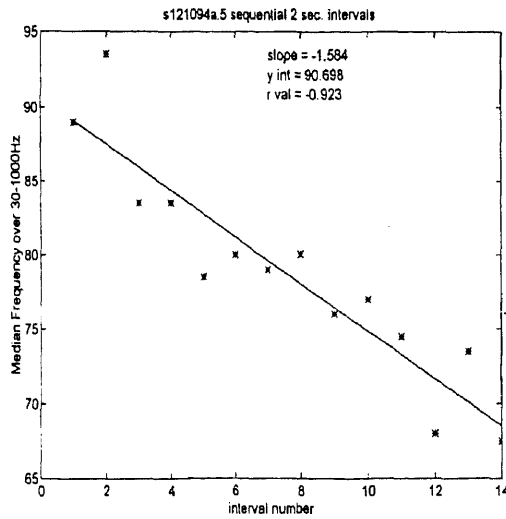
This section documents the results from a pilot study obtained by testing six subjects with no prior neuromuscular diseases. Each subject was tested as per the protocol discussed in section 2.2.2. The eight channels of simultaneous recording of EMG signals were processed for median frequency, mean frequency and root mean square computations. These parameters were subjected to linear regression and correlation coefficient calculations to obtain slope, y-intercept and correlation coefficient.

The slope, y intercept and correlation coefficient values of median, mean , and rms values of all 4 trials for all the subjects is listed in table 3.4, table 3.5 and table 3.6 in Appendix A respectively. Recalling the objective of this study, channels 1 (SA-SR), 2 (FW1-FW2), 3 (FW2-FW3), 4 (FW1-FW2), 5 (FW1-SA) and 6 (FW1-SR) were of interest in order to compare monopolar fine wire (5 and 6) with surface (1) and bipolar fine wire (2). A crude analysis was done to find the range of initial median frequency , initial mean frequency and their corresponding slope for each of these channels from the data whose correlation coefficient was 0.5 or better. This range of values has been summarized in table 3.7.

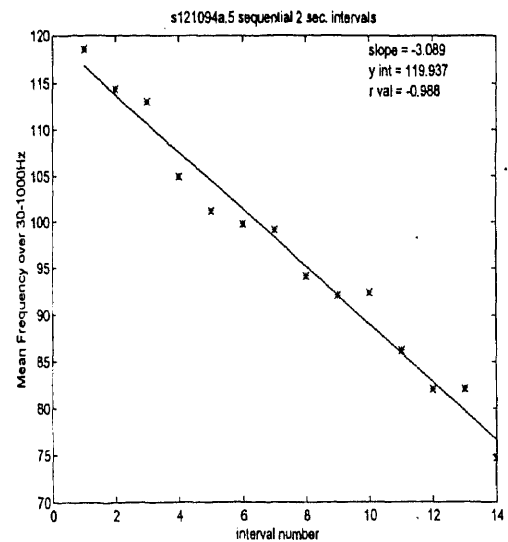
Figure 3.4 A shows a least square line fit to median frequency data for subject 1, trial 1, monopolar fine wire (FW1-SA) and B shows the least square fit to the mean frequency for the same subject. Figure 3.5 A shows a least square line fit to the rms data for the same subject and B shows subject 3, trial 1 for monopolar fine wire (FW1-SA) (a poor fit).

Table 3.7 Range of values for y intercept and slope of median and mean frequency.

Channel (channel no)	Median Frequency		Mean Frequency	
	Initial median frequency	Slope	Initial mean frequency	Slope
(1) SA-SR	57 to 89	-0.42 to -1.9	61 to 105	-0.33 to -1.6
(2) FW1-FW2	110 to 210	-0.8 to -4.5	143.8 to 236	-1.5 to -5.2
(3) FW2-FW3	82 to 138	-1.6 to -3.0	113.0 to 178.4	-0.88 to -4.0
(4) FW1-FW3	78 to 120	-0.45 to -2.8	108 to 144	-0.89 to -2.97
(5) FW1-SA	80 to 125	-0.5 to -3.2	107.6 to 191.7	-0.955 to -3.9
(6) FW1-SR	87 to 131	-0.52 to -2.5	106 to 164.9	-0.86 to -4.16



A



B

Figure 3.4 A. Least square fit to median frequency data: good fit subject 1, trial 1, monopolar fine wire; B. Least square fit to mean frequency for the same subject.

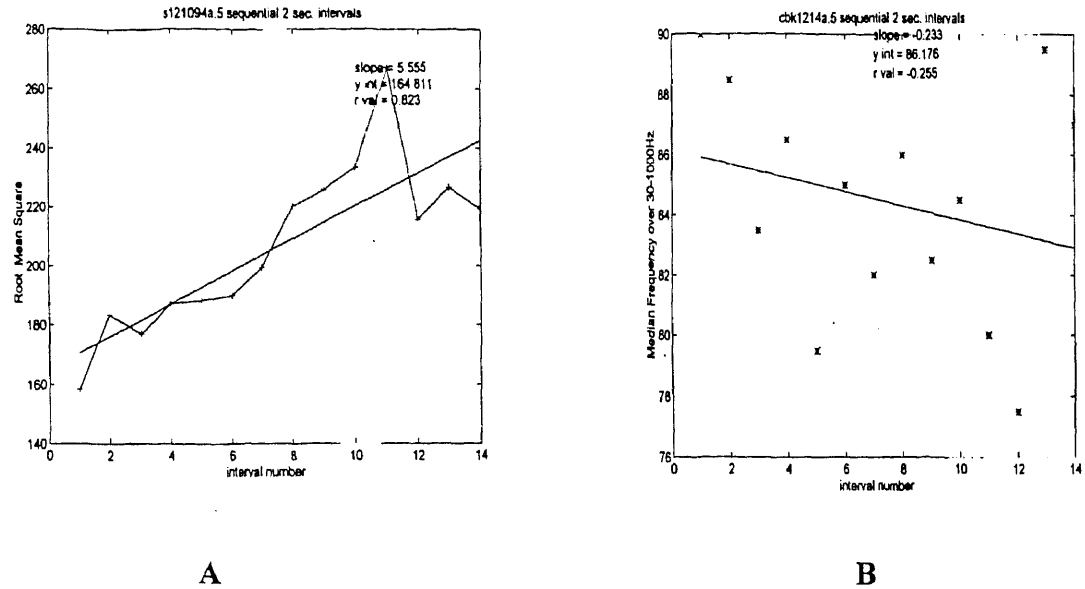


Figure 3.5 A. Least square fit to rms data: good fit subject 1, trial 1, monopolar fine wire; B. Least square fit to median frequency data poor fit subject 3, trial 1 for monopolar fine wire.

The rms values were not taken into consideration because we obtained ambiguous results which varied from subject to subject. Considering subjects 1,5 and 6 in table 3.6 the rms value increases with fatigue (slope is positive) for all the trials and for all the channels but it decreases with fatigue in the other subjects. In all the subjects the initial median frequency for monopolar fine wire referenced to surface active (FW1-SA (5)) has a value less than bipolar fine wire (FW1-FW2) but greater than surface electrodes for all data points where the correlation coefficient was 0.5 or higher. The slope showed a similar trend except for subjects 2 and 3 where the slope value of the surface electrodes was greater than that of monopolar fine wire. However the initial mean frequency and the slope of monopolar fine wire were greater than those of the surface electrode but less

than the bipolar fine wire (FW1-FW2) in all the subjects. This argument can be easily understood by comparing values between channels 1, 2 and 5 in Table 3.7 in Appendix A. See Appendix E for power analysis computations for both groups.

CHAPTER 4

DISCUSSION AND CONCLUSIONS

4.1 Discussion and conclusions for Group I

Before performing the actual pilot study, a comparison was made of the initial median frequency value obtained from simultaneously recording of EMG signals from the Delsys and the Teca electrodes. We saw a higher initial median frequency values for the Delsys electrode in most of the cases. This suggests that despite the of low pass filtering effect of the skin, the Delsys electrode, because of its built in circuitry, picks up higher frequency components of the EMG signal than the Teca electrode indicating better frequency response.

In the experimental study the normal median frequency and slope (fatigue index) values obtained for 3 muscles based on data from 6 subjects as follows:

Biceps initial median frequency: 59.2 Hz to 144.4 Hz

 slope: -1.6 to -0.3

Triceps initial median frequency 72.0 Hz to 98.0 Hz

 slope -1.2 to -0.07

Deltoid initial median frequency 72.1 to 122.5 Hz

 slope -1.78 to -0.18.

The results of non parametric ANOVA listed in the previous chapter showed no significant difference in the initial median frequency and slope between the three

muscles. However, these values were based on only few subjects and we may see significant differences when testing all 62 subjects.

Although the results do not show significant differences, trends in the data suggest the following possible discussion. The value obtained for slope suggests that triceps fatigues less compared to equal fatiguing of biceps and deltoid. This observation suggests that the amount of type I fiber (most fatigue resistant) is greater in the triceps compared to the other two. However, this observation is contrary to another study by Johnson, Polgar, et al [22] on distribution of fiber types in human muscles suggesting less number of type I fibers in triceps compared to both biceps and deltoid. However, our results were based on only six subjects and to validate this result and to establish normal median frequency values a power analysis (Appendix E) showed 62 subjects were needed to consider the study both clinically and statistically significant.

From the result, it was also observed that a lower correlation coefficient was obtained when the subject was unable to maintain a steady force level. Though we took the mean of the three trials to calculate a single mean and slope value of a subject for each muscle no consideration was made for variation in the force level. The author suggests that the force signal needs to be further processed to decide between good data and bad data. One such processing system that can be considered has the following steps:

1. Calculate the average value of the force level maintained by the subject during his contraction (\bar{X}).
2. Define the range(low (a) - high (b)) between which the mean value should lie in order to consider whether the data is good or bad .

3. Compute the deviation of force from the mean for every instant of time.
4. Estimate standard deviation (SD) of the deviated values.
5. Compute 95% confidence interval ($\bar{X} \pm 2SD$).
6. Check to see if the original force values lie within the 95% confidence interval.
7. The data within these confidence interval will be considered as good data.

This whole sequence can be well understood by the flow chart shown in Figure 4.1.

Admittedly, this algorithm has to be tested and if it fails then another method of processing force will have to be developed.

In conclusion, once the normal median frequency values for the upper extremity muscles become available based on the data from 62 subjects, spectral analysis can be used clinically to evaluate patients with fatigue producing diseases such as chronic fatigue syndrome, multiple sclerosis, myopathies, neuropathies, and motor neuron disease by comparing the median frequency values with the normal. Further, this study will enhance the current clinical EMG evaluations by proposing a new technique to study fatigue by testing muscles using a hand held dynamometer, manual muscle testing techniques, and standard processing equipment.

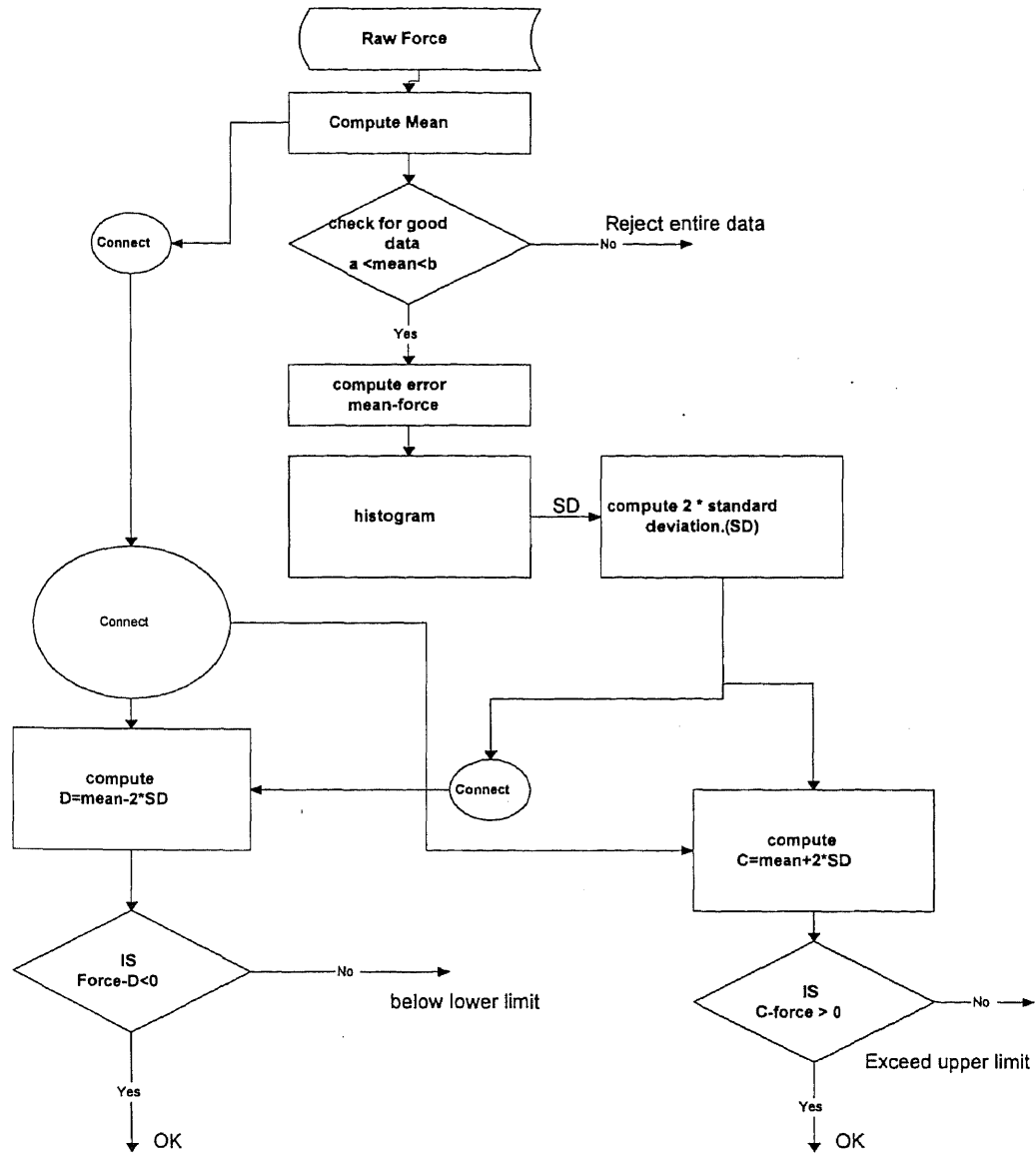


Figure 4.1 shows flow chart for processing force. a and b represent the lower and the higher values respectively for accepting data as good data.

4.2 Discussion and Conclusions for Group II

The objective of this study was to determine whether a single fine wire as the active electrode referenced to a surface electrode (monopolar fine wire) can validly and reliably measure muscle fatigue; and to determine if monopolar fine wire is equivalent to or better than a bipolar surface electrode. Another objective was to determine what distance between two bipolar fine wires consistently and reliably detects fatigue. Having placed the electrode on the biceps as shown in figure 2.1 and testing the different combinations (refer table 2.1) at the same time for 30 sec duration gave the results as discussed in chapter 3.

Monopolar fine wire, that is fine wire 1 as the active electrode referenced to the active electrode of the surface bar electrode (FW1-SA), showed a higher value of initial median frequency and initial mean frequency as compared to the surface electrode. It was also observed that except for two subjects, the slope (fatigue index) values of monopolar fine wire was higher than bipolar surface electrodes when median frequency was the parameter under study and for all the subjects with mean frequency. This higher value of y intercept, which is the measure of initial median frequency and slope, which is an indicator of the amount of fatigue of the muscle, indicates that monopolar fine wire because of its higher slope value may be better than a bipolar surface electrode for measuring fatigue via mean and median frequency. This higher slope value may be reflection of accurate frequency response and accurate positioning of monopolar fine wire electrode with respect to the motor point.

Recall that we had 3 bipolar fine wire configurations: fine wire 1 (FW1) referenced to fine wire 2 (FW2) that is (FW1-FW2), as well as (FW2-FW3) and (FW1-FW3), and we found that the initial median frequency, mean frequency and slope for monopolar fine wire (FW1-SA) was less than bipolar fine wire (FW1-FW2) for all the subjects. However, when the initial median frequency, mean frequency and slope of monopolar fine wire were compared with that of the other two bipolar fine wire (FW2-FW3) and (FW1-FW3), we observed that parameters were higher for monopolar than that of both bipolar in some of the subjects and vice versa in others. The amount of differences should be tested statistically by non parameteric analysis of variance (ANOVA).

Referring to figure 2.1 and recalling the distances between three fine wire FW1, FW2, FW3, We compared the slopes (fatigue index) of all the three bipolar fine wire (FW1-FW2), (FW2-FW3) and (FW1-FW3) in order to test our third objective as to what distance between two bipolar fine wire consistently and reliably detects fatigue. It was observed that the slope of bipolar (FW1-FW2) was higher than that of the other two bipolar electrodes but the slope of FW1-FW3 was lower in most of the subjects as compared to FW2-FW3. The possible discussion to this difference could be that FW1-FW2 (1 cms apart) showed greater fatigue as compared to FW2-FW3 and FW1-FW2 because of FW1 being closer to motor point. However, despite FW1 being more proximal to motor point than FW2, the slope indicated by FW1 and FW3 separated 2 cms apart showed less fatigue compared to FW2 and FW3 separated 1 cms apart. This suggests that as far as bipolar fine wire is concerned apart from the proximity of the electrode to motor

point the distance between the electrode to which it is referenced is also important in order to reliably measure fatigue.

Referring back to table 3.2 and figure 2.1 we have 3 combinations of monopolar fine wire electrodes (FW1-SA), (FW1-SR) and (FW3-SR) , We observed that the initial frequency and slope values for monopolar fine wire (FW1-SR and FW1-SA) were higher than monopolar fine wire (FW3-SR). This observation suggests that although the distance between the fine wire electrode (FW3) and the surface reference (SR) was less than the distance between FW1 and SR, the fatigue indicated by FW3-SR was less than that indicated by FW1-SR or FW1-SA. One possible explanation is that as far as monopolar fine wire is concern the electrode with respect to the motor point and not the distance between the electrodes reliably measure fatigue.

The bipolar fine wire (FW1-FW3) and (FW3-FW1) showed almost similar values for initial frequency and slope values rendering one of the channels redundant. It appears that the results from monopolar fine wire (FW1-SA) and (FW1-SR) have to be tested statistically to see if there exists any significant differences between their intercepts and slope values.

Table 4.1 shows the slope, y intercept and the correlation coefficient of median frequency for all the trials of subject 1. Looking at table 4.1 and comparing trials 1 and 2 or trials 3 and 4 for intratest reliability and comparing trials 1 and 3, it appears that slope and the y intercept values has to be tested statistically. For further comparison reference to tables 3.4 and 3.5 in Appendix A is suggested..

The RMS values for different channels were very much inconsistent among subjects. It has been reported that RMS value increases over time for surface electrodes and decreases over time for cannula electrodes [1]. This increase in RMS value over time for surface electrodes was observed only in subject 1, 5 and 6 . The RMS value for bipolar fine wire increased for subjects 1,5 and 6 and decreased over time for other subjects. Results indicated good correlation values of mean and median frequency inspite of lower correlation (< 0.5) in RMS value. One such example is the results from subject 2. Due to such ambiguity in results the investigators of this group are considering not using this parameter as an indicator of fatigue for the remaining subjects. The results of this study needs to be validated by testing a minimum of 29 subjects, estimated by power analysis (See Appendix E), with correlation coefficient of 0.5 or better.

Table 4.1 shows the slope, intercept and the correlation coefficient of median frequency from regression and correlation analysis.

Channel	Median Frequency Parameters	Subject 1			
		Trial #			
		1	2	3	4
1 (SA-SR)	slope	-0.845	-1.158	-1.92	-1.84
	y intercept	57.3	60.1	69.1	65.4
	corr coeff	-0.860	-0.841	-0.843	-0.799
2 (FW1-FW2)	slope	-3.615	-3.258	-4.538	-4.389
	y intercept	117.5	116.5	177.7	150.9
	corr coeff	-0.971	-0.968	-0.96	-0.982
3 (FW2-FW3)	slope	-1.888	-2.310	-3.004	-2.369
	y intercept	85.5	82.8	127.8	95.269
	corr coeff	-0.941	-0.952	-0.952	-0.843
4 (FW1-FW3)	slope	-1.913	-2.059	-2.799	-1.760
	y intercept	87.1	86.8	106.4	90.8
	corr coeff	-0.958	-0.936	-0.957	-0.915
5 (FW1-SA)	slope	-1.584	-1.87	-2.631	-2.874
	y intercept	90.7	91.0	122.6	125.0
	corr coeff	-0.923	-0.949	-0.987	-0.971
6 (FW1-SR)	slope	-2.469	-2.138	-2.413	-1.965
	y intercept	91.1	89.7	123.67	116.7
	corr coeff	-0.927	-0.973	-0.98	-0.904

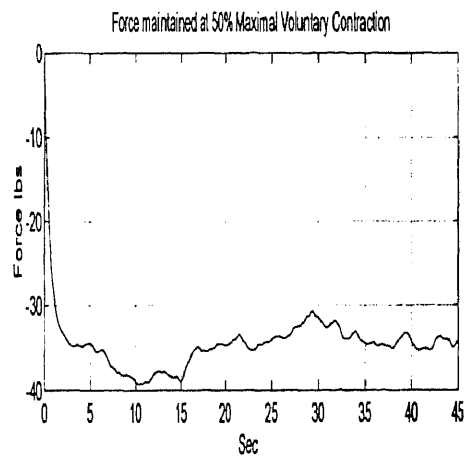
In conclusion it appears that monopolar fine wire can be used to reliably measure fatigue but this argument can be validated only after testing 29 subjects. Statistical analysis will be performed at that time, using ANOVA.

4.3 Suggestions for Future Work

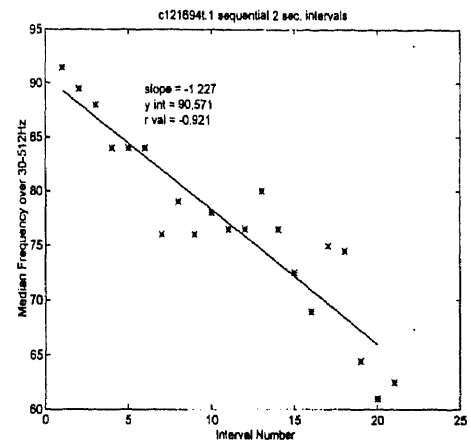
For group I, as discussed in section 4.1, the force signal has to be further processed as it was observed that variation in force levels had significant effect on correlation coefficient values and also, at times, results showed a good correlation despite large force variation produced by the subject. An example of this is shown in figure 4.2. This suggests that the force signal has to be further processed and one such processing system was discussed in section 4.1 but was not tested.

For group II, although signals from 8 channels are presently being recorded, it is clear from this study that some of the channels (FW1-FW3) and (FW3-FW1) are redundant. By reducing the number of channels, the number of cables and in turn the interference from instrumentation noise will be reduced.

Sometimes inconsistency in data has been observed when using fine wire electrodes and retesting the subject. This may be due to dislodging of fine wire electrodes between the first and the second session. Therefore the signal from the fine wire electrodes must be tested before actual acquisition is made. One recommendation is to test the channels with the Dantech EMG monitoring equipment as it has an acoustic output in response to the firing motor unit.



A



B

Figure 4.2 A. shows the force maintained at 50 % MVC showing large variation in force level; B shows corresponding least square fit to median frequency.

APPENDIX A

**TABLES OF MEDIAN FREQUENCY, MEAN FREQUENCY AND ROOT MEAN
SQUARE OF GROUP II**

Table 3.4 Shows the slope, Y intercept and the correlation coefficient of **median** frequency from regression and correlation analysis.

Channel	Median Frequency Parameters	Subject 1				Subject 2				Subject 3			
		Trial #				Trial #				Trial #			
		1	2	3	4	1	2	3	4	1	2	3	4
1 (SA-SR)	slope	-0.845	-1.158	-1.92	-1.84	-1.784	-1.899	-1.064	-1.064	-0.804	-0.787	-1.373	-1.08
	y intercept	57.3	60.1	69.1	65.4	74.1	74.1	77.1	75.3	60.9	59.3	69.8	64.2
	corr coeff	-0.860	-0.841	-0.843	-0.799	-0.789	-0.935	-0.834	-0.842	-0.48	-0.783	-0.688	-0.681
2 (FW1-FW2)	slope	-3.615	-3.258	-4.538	-4.389	-2.832	-2.695	-4.125	-3.091	-1.541	-1.631	-2.004	-1.488
	y intercept	117.5	116.5	177.7	150.9	192.3	200.5	200.2	164.3	110.9	185.7	182.7	169.5
	corr coeff	-0.971	-0.968	-0.96	-0.982	-0.906	-0.950	-0.928	-0.936	-0.194	-0.757	-0.929	-0.805
3 (FW2-FW3)	slope	-1.888	-2.310	-3.004	-2.369	-2.393	-2.638	-1.877	-1.756	-1.402	-0.815	-1.63	-1.986
	y intercept	85.5	82.8	127.8	95.269	138.2	125.8	116.7	115.7	93.0	120.3	122.0	124.0
	corr coeff	-0.941	-0.952	-0.952	-0.843	-0.942	-0.935	-0.953	-0.8	-0.321	-0.424	-0.757	-0.942
4 (FW1-FW3)	slope	-1.913	-2.059	-2.799	-1.760	-1.8	-2.165	-1.822	-1.682	-0.978	-0.909	-0.836	-1.327
	y intercept	87.1	86.8	106.4	90.8	120.6	116.3	117.7	113.1	94.2	89.6	99.7	102.5
	corr coeff	-0.958	-0.936	-0.957	-0.915	-0.919	-0.954	-0.942	-0.861	-0.616	-0.653	-0.568	-0.78
5 (FW1-SA)	slope	-1.584	-1.87	-2.631	-2.874	-1.267	-1.445	-1.622	-1.955	-0.233	-0.509	-1.012	-1.22
	y intercept	90.7	91.0	122.6	125.0	92.5	110.2	105.4	113.6	86.2	82.1	97.1	97.7
	corr coeff	-0.923	-0.949	-0.987	-0.971	-0.872	-0.937	-0.926	-0.933	-0.255	-0.548	-0.5	-0.53
6 (FW1-SR)	slope	-2.469	-2.138	-2.413	-1.965	-1.887	-1.921	-2.4	-2.21	-1.142	-0.94	-0.844	-0.871
	y intercept	91.1	89.7	123.67	116.7	128.8	116.82	131.3	123.0	125.0	114.9	101.8	102.4
	corr coeff	-0.927	-0.973	-0.98	-0.904	-0.873	-0.934	-0.929	-0.937	-0.608	-0.622	-0.712	-0.668
7 (FW3-SR)	slope	-1.268	-1.073	-1.21	-0.999	-1.501	-1.285	-1.504	-1.240	-0.851	-0.644	-0.603	-0.949
	y intercept	64.9	59.3	71.5	66.7	85.3	77.4	86.7	83.2	68.3	66.8	70.4	72.8
	corr coeff	-0.809	-0.832	-0.796	-0.858	-0.847	-0.882	-0.903	-0.859	-0.849	-0.768	-0.642	-0.694
8 (FW3-FW1)	slope	-1.933	-2.092	-2.824	-1.788	-1.766	-1.851	-1.778	-1.667	-1.008	-0.91	-1.199	-1.444
	y intercept	87.7	87.7	107.2	91.7	121.2	122.0	117.9	113.3	95.4	90.6	113.7	113.5
	corr coeff	-0.956	-0.938	-0.959	-0.917	-0.921	-0.938	-0.942	-0.859	-0.624	-0.649	-0.695	-0.879

Table 3.4 (continued from last page)

Channel	Median Frequency Parameters	Subject 4				Subject 5				Subject 6			
		Trial #				Trial #				Trial #			
		1	2	3	4	1	2	3	4	1	2	3	4
1 (SA-SR)	slope	-0.665	-0.818	-0.635	-0.792	-0.285	-0.352	-0.696	-0.915	-0.833	-0.426	-0.308	0.896
	y intercept	73.7	75.9	76.2	84.4	63.2	63.4	76.1	89.0	79.2	73.9	57.1	59.3
	corr coeff	-0.679	-0.876	-0.756	-0.854	-0.481	-0.421	-0.575	-0.701	-0.776	-0.621	-0.248	-0.712
2 (FW1-FW2)	slope	-1.227	-0.658	-1.518	-1.976	-3.044	-3.016	-2.352	-2.784	-0.925	-4.475	-2.927	-3.577
	y intercept	150.5	147.3	138.1	147.0	204.2	192.4	130.6	159.2	157.4	160.8	210.5	193.3
	corr coeff	-0.608	-0.45	-0.883	-0.932	-0.920	-0.903	-0.897	-0.918	-0.228	-0.893	-0.948	-0.940
3 (FW2-FW3)	slope	-2.907	-1.034	-1.321	-1.886	-2.796	-2.303	-0.463	-0.331	0.296	-1.388	-0.611	-0.867
	y intercept	123.3	108.9	123.1	136.4	145.2	136.1	97.1	92.4	85.104	101.6	103.9	101.7
	corr coeff	-0.818	-0.448	-0.717	-0.843	-0.858	-0.778	-0.427	-0.248	0.167	-0.845	-0.389	-0.664
4 (FW1-FW3)	slope	-0.527	-0.998	-0.911	-0.716	-1.046	-0.959	-0.458	-0.274	-1.253	-1.440	-0.243	-0.697
	y intercept	107.9	104.1	88.2	78.0	102.6	104.2	86.6	86.5	106.2	105.7	86.9	84.7
	corr coeff	-0.839	-0.601	-0.793	-0.589	-0.844	-0.581	-0.519	-0.225	-0.847	-0.858	-0.205	-0.545
5 (FW1-SA)	slope	-0.920	-1.049	-0.965	-3.281	-1.120	-1.087	-1.026	-0.678	-1.823	-1.887	-2.148	-3.112
	y intercept	135.2	133.8	108.4	108.9	105.4	105.3	92.9	99.2	135.6	124.7	152.3	151.7
	corr coeff	-0.763	-0.840	-0.653	-0.814	-0.561	-0.719	-0.712	-0.398	-0.891	-0.909	-0.905	-0.973
6 (FW1-SR)	slope	-0.522	-0.982	-0.725	-1.007	-1.136	-1.648	-1.258	-1.040	-1.443	-1.749	-1.541	-0.960
	y intercept	118.2	117.0	90.2	87.1	110.6	123.6	103.6	109.9	116.9	108.3	123.2	114.6
	corr coeff	-0.592	-0.858	-0.785	-0.907	-0.663	-0.865	-0.836	-0.762	-0.919	-0.889	-0.668	-0.690
7 (FW3-SR)	slope	-1.49	-1.148	-0.637	-0.257	-0.499	-0.277	-0.204	-0.370	-0.349	-0.501	-0.033	-0.710
	y intercept	87.6	85.07	76.7	76.2	79.0	74.7	76.4	75.7	72.8	73.0	76.5	80.538
	corr coeff	-0.907	-0.860	-0.781	-0.283	-0.503	-0.249	-0.236	-0.416	-0.411	-0.560	-0.073	-0.657
8 (FW3-FW1)	slope	-0.553	-1.007	-0.922	-0.693	-1.066	-1.022	-0.493	-0.244	-1.240	-1.459	-0.249	-0.726
	y intercept	108.5	105.1	88.7	78.3	103.7	105.7	87.4	86.7	106.9	106.5	87.9	85.8
	corr coeff	-0.414	-0.636	-0.805	-0.584	-0.867	-0.638	-0.557	-0.198	-0.846	-0.873	-0.196	-0.575

Table 3.5 shows the slope, y intercept and the correlation coefficient of mean frequency from regression analysis.

Channel	Mean Frequency Parameters	Subject 1				Subject 2				Subject 3			
		Trial #				Trial #				Trial #			
		1	2	3	4	1	2	3	4	1	2	3	4
1 (SA-SR)	slope	-0.875	-1.270	-1.659	-1.99	-1.242	-1.299	-1.180	-1.216	-0.575	-0.49	-0.899	-0.455
	y intercept	68.6	71.4	81.0	80.5	81.3	79.6	86.5	86.12	75.7	72.8	78.3	76.5
	corr coeff	-0.842	-0.952	-0.938	-0.935	-0.862	-0.972	-0.938	-0.924	-0.588	-0.718	-0.821	-0.653
2 (FW1-FW2)	slope	-5.283	-4.404	-5.169	-4.839	-3.118	-3.083	-5.165	-3.523	-1.625	-1.574	-2.519	-2.068
	y intercept	151.7	143.8	217.3	179.9	227.5	230.6	236.3	187.0	165.9	209.7	211.0	197.7
	corr coeff	-0.986	-0.986	-0.987	-0.985	-0.93	-0.950	-0.933	-0.961	-0.354	-0.77	-0.934	-0.918
3 (FW2-FW3)	slope	-3.302	-3.484	-4.058	-3.291	-2.957	-2.586	-2.279	-1.859	-1.818	-0.822	-1.828	-2.056
	y intercept	119.8	113.8	163.4	143.7	165.1	147.5	134.7	129.5	135.4	150.0	150.5	147.6
	corr coeff	-0.982	-0.969	-0.987	-0.943	-0.962	-0.962	-0.971	-0.891	-0.533	-0.504	-0.853	-0.908
4 (FW1-FW3)	slope	-2.973	-2.927	-3.138	-2.288	-1.992	-1.968	-2.781	-2.249	-1.116	-1.302	-1.0	-1.382
	y intercept	117.5	108.5	131.0	115.6	136.3	127.4	144.1	137.0	130.4	134.8	118.6	119.2
	corr coeff	-0.984	-0.966	-0.975	-0.977	-0.952	-0.954	-0.938	-0.906	-0.633	-0.705	-0.754	-0.897
5 (FW1-SA)	slope	-3.089	-2.76	-3.089	-3.152	-1.378	-1.459	-2.365	-2.348	-0.188	-1.131	-1.194	-1.271
	y intercept	119.9	112.3	141.1	137.9	107.6	118.9	129.5	133.8	116.8	118.8	112.2	112.1
	corr coeff	-0.988	-0.976	-0.991	-0.985	-0.907	-0.955	-0.932	-0.945	-0.167	-0.726	-0.631	-0.704
6 (FW1-SR)	slope	-4.161	-3.215	-3.236	-2.806	-2.114	-1.848	-3.355	-2.449	-0.588	-1.413	-0.960	-0.864
	y intercept	121.1	111.9	151.8	139.7	141.5	127.3	159.3	144.8	146.9	153.5	117.1	115.4
	corr coeff	-0.98	-0.984	-0.992	-0.953	-0.937	-0.94	-0.943	-0.940	-0.433	-0.833	-0.878	-0.877
7 (FW3-SR)	slope	-1.970	-1.067	-2.039	-1.123	-1.481	-1.688	-1.482	-1.296	-0.967	-0.630	-0.733	-1.345
	y intercept	89.1	72.8	99.1	86.7	104.3	99.2	101.4	100.1	89.31	85.0	94.9	100.5
	corr coeff	-0.938	-0.906	-0.9	-0.988	-0.874	-0.957	-0.944	-0.832	-0.748	-0.697	-0.672	-0.822
8 (FW3-FW1)	slope	-3.017	-2.945	-3.157	-2.296	-1.99	-1.899	-2.799	-2.266	-1.117	-1.309	-1.175	-1.496
	y intercept	118.7	109.3	132.0	116.5	137.0	134.8	145.1	137.8	131.8	136.3	129.1	128.0
	corr coeff	-0.985	-0.966	-0.976	-0.977	-0.953	-0.948	-0.936	-0.906	-0.636	-0.71	-0.835	-0.919

Table 3.5 (continued from last page)

Channel	Mean Frequency Parameters	Subject 4				Subject 5				Subject 6			
		Trial #				Trial #				Trial #			
		1	2	3	4	1	2	3	4	1	2	3	4
1 (SA-SR)	slope	-0.546	-0.637	-0.753	-0.999	-0.325	-0.440	-0.891	-0.794	-1.254	-0.867	-0.400	-0.730
	y intercept	79.9	82.5	84.1	92.6	70.4	71.3	95.9	105.1	94.3	87.5	68.0	68.7
	corr coeff	-0.762	-0.842	-0.895	-0.927	-0.515	-0.657	-0.858	-0.710	-0.898	-0.871	-0.687	-0.807
2 (FW1-FW2)	slope	-2.176	-0.897	-1.839	-2.036	-3.138	-3.128	-3.877	-3.391	0.390	-3.953	-3.187	-4.227
	y intercept	181.4	179.0	156.2	168.8	226.2	214.8	181.7	203.1	186.4	205.9	232.8	217.5
	corr coeff	-0.865	-0.558	-0.9	-0.955	-0.939	-0.928	-0.957	-0.946	0.120	-0.919	-0.972	-0.963
3 (FW2-FW3)	slope	-3.631	-1.088	-1.608	-1.563	-2.568	-2.336	-1.406	-1.112	0.474	-2.014	-1.529	-1.753
	y intercept	159.4	144.0	143.6	154.9	178.4	170.0	138.3	128.7	107.8	131.9	147.6	137.6
	corr coeff	-0.870	-0.437	-0.901	-0.891	-0.921	-0.882	-0.821	-0.722	0.222	-0.950	-0.787	-0.907
4 (FW1-FW3)	slope	-1.318	-0.890	-1.096	-1.567	-1.456	-1.309	-1.965	-1.475	-1.466	-1.945	-1.435	-1.643
	y intercept	135.6	129.1	109.6	113.1	132.3	137.8	132.6	129.6	139.1	136.3	137.0	127.2
	corr coeff	-0.789	-0.695	-0.889	-0.785	-0.885	-0.747	-0.890	-0.869	-0.838	-0.956	-0.798	-0.838
5 (FW1-SA)	slope	-1.344	-1.075	-0.955	-2.712	-1.700	-1.994	-2.643	-1.608	-2.592	-2.804	-3.151	-3.931
	y intercept	154.8	153.5	119.3	136.0	130.8	138.3	135.7	134.7	169.8	158.7	191.7	185.4
	corr coeff	-0.844	-0.848	-0.745	-0.845	-0.707	-0.891	-0.898	-0.763	-0.960	-0.968	-0.938	-0.983
6 (FW1-SR)	slope	-1.086	-0.977	-0.96	-1.558	-1.702	-2.193	-3.019	-2.697	-1.819	-2.224	-2.670	-1.666
	y intercept	141.8	139.6	109.0	106.6	139.5	154.6	155.9	161.3	145.5	133.8	164.9	147.8
	corr coeff	-0.811	-0.815	-0.906	-0.944	-0.888	-0.904	-0.947	-0.936	-0.944	-0.933	-0.922	-0.920
7 (FW3-SR)	slope	-1.572	-1.106	-0.836	-0.451	-0.722	-0.306	-0.029	-0.649	-0.814	-0.808	0.216	-0.680
	y intercept	103.9	101.6	90.7	91.9	105.5	102.1	95.3	97.6	104.6	102.9	91.5	95.1
	corr coeff	-0.93	-0.884	-0.916	-0.590	-0.528	-0.199	-0.030	-0.660	-0.568	-0.728	0.309	-0.732
8 (FW3-FW1)	slope	-1.329	-0.897	-1.092	-1.586	-1.481	-1.325	-2.013	-1.520	-1.473	-1.962	-1.464	-1.666
	y intercept	136.6	130.2	110.3	114.4	13305	139.1	134.2	131.1	140.3	137.4	138.7	128.5
	corr coeff	-0.791	-0.701	-0.886	-0.785	-0.886	-0.752	-0.894	-0.869	-0.837	-0.956	-0.804	-0.840

Table 3.6 shows the slope, y intercept and the correlation coefficient of **root mean square (RMS)** from regression analysis.

Channel	RMS Parameters	Subject 1				Subject 2				Subject 3			
		Trial #				Trial #				Trial #			
		1	2	3	4	1	2	3	4	1	2	3	4
1 (SA-SR)	slope	6.053	7.129	1.064	0.907	-1.070	-0.728	-2.857	-2.783	-1.756	-0.793	-0.071	-0.046
	y intercept	88.1	94.7	21.1	25.7	138.2	75.5	421.4	431.6	74.8	66.6	42.0	48.9
	corr coeff	0.97	0.926	0.960	0.848	-0.308	-0.436	-0.326	-0.32	-0.738	-0.337	-0.049	-0.019
2 (FW1-FW2)	slope	6.807	6.49	2.169	1.321	-2.276	-3.170	-1.856	-0.127	-10.98	-2.325	-0.245	-1.179
	y intercept	165.3	173.2	54.7	51.9	211.2	197.6	155.8	207.2	314.8	77.7	48.4	66.0
	corr coeff	0.861	0.899	0.903	0.798	-0.477	-0.735	-0.587	-0.030	-0.568	-0.650	-0.291	-0.631
3 (FW2-FW3)	slope	4.310	2.694	0.815	0.485	-3.502	-1.408	-0.731	-0.843	-6.808	-1.644	-0.154	-1.539
	y intercept	178.8	60.4	20.4	14.3	317.0	119.7	228.5	251.2	207.3	55.7	66.7	95.8
	corr coeff	0.891	0.919	0.8	0.852	-0.479	-0.561	-0.133	0.178	-0.545	-0.664	-0.159	-0.54
4 (FW1-FW3)	slope	2.696	1.843	1.096	0.971	0.474	-1.388	-1.115	-1.023	-0.563	-0.155	0.169	-0.761
	y intercept	98.9	39.0	32.5	29.4	74.6	249.0	267.2	271.4	28.6	19.3	56.0	70.323
	corr coeff	0.801	0.905	0.859	0.915	0.29	-0.289	-0.17	-0.196	-0.751	-0.491	0.157	-0.499
5 (FW1-SA)	slope	5.555	7.138	1.827	1.598	-0.175	-1.352	-1.849	-1.293	-0.563	-0.410	0.217	-0.419
	y intercept	164.8	171.8	59.3	49.2	102.9	113.4	308.7	287.8	28.6	44.085	57.4	71.1
	corr coeff	0.823	0.881	0.817	0.879	-0.073	-0.491	-0.245	-0.21	-0.751	-0.376	0.235	-0.275
6 (FW1-SR)	slope	9.741	10.484	0.729	1.496	0.296	-1.027	-1.040	-1.4	-0.577	-0.149	0.023	-1.014
	y intercept	148.1	159.7	22.233	33.5	75.2	106.5	140.2	159.8	21.5	14.0	58.8	74.7
	corr coeff	0.925	0.922	0.8	0.914	0.174	-0.398	-0.283	-0.375	-0.837	-0.506	0.02	-0.533
7 (FW3-SR)	slope	5.846	2.609	1.574	1.07	0.253	0.641	0.59	-0.126	0.154	-0.160	0.491	0.6
	y intercept	112.1	39.493	55.7	69.8	44.5	41.8	135.9	142.1	58.82	56.6	102.0	113.9
	corr coeff	0.963	0.974	0.921	0.691	0.532	0.774	0.345	-0.088	0.166	-0.178	0.418	0.595
8 (FW3-FW1)	slope	4.641	3.327	1.128	1.004	0.395	-0.781	-1.178	-1.062	-0.574	-0.162	0.430	-1.845
	y intercept	182.2	72.1	34.4	31.6	75.2	94.9	268.9	272.7	30.0	20.6	130.3	165.2
	corr coeff	0.806	0.902	0.863	0.911	0.245	-0.409	-0.179	-0.203	-0.749	-0.489	0.160	-0.504

Table 3.6 (continued from last page)

Channel	RMS Parameters	Subject 4				Subject 5				Subject 6			
		Trial #				Trial #				Trial #			
		1	2	3	4	1	2	3	4	1	2	3	4
1 (SA-SR)	slope	-0.688	-0.063	0.427	0.732	9.419	5.808	2.179	2.459	6.205	4.005	1.302	0.755
	y intercept	42.6	35.6	73.5	62.5	206.7	231.7	86.1	76.0	95.4	148.9	18.2	27.8
	corr coeff	-0.581	-0.095	0.389	0.427	0.745	0.692	0.732	0.671	0.926	0.698	0.900	0.718
2 (FW1-FW2)	slope	0.282	0.107	0.252	2.216	2.039	0.139	1.925	0.451	-0.498	-1.118	0.226	1.678
	y intercept	43.6	32.3	84.6	75.8	133.4	157.0	151.2	54.3	115.8	115.7	41.1	36.3
	corr coeff	0.197	0.167	0.281	0.748	0.763	0.139	0.560	0.473	-0.101	-0.307	0.153	0.512
3 (FW2-FW3)	slope	0.470	0.198	-0.246	0.837	1.738	0.761	2.715	0.119	5.430	1.960	0.362	1.092
	y intercept	24.5	18.2	81.9	77.7	99.4	115.6	141.7	64.7	110.7	145.2	24.6	25.1
	corr coeff	0.414	0.592	-0.317	0.524	0.812	0.438	0.566	0.088	0.764	0.555	0.384	0.530
4 (FW1-FW3)	slope	-0.289	-0.071	0.812	2.375	1.957	1.159	3.445	0.971	1.909	1.543	0.542	0.450
	y intercept	23.5	21.6	50.6	41.1	69.1	78.1	168.4	60.2	63.4	64.7	13.8	17.8
	corr coeff	-0.633	-0.192	0.425	0.754	0.850	0.799	0.705	0.580	0.907	0.839	0.908	0.889
5 (FW1-SA)	slope	-0.629	-0.131	0.686	2.420	1.164	0.548	1.731	1.366	3.729	2.369	0.854	0.779
	y intercept	40.3	35.0	48.3	36.6	30.4	35.5	68.4	60.7	84.0	91.7	20.3	24.8
	corr coeff	-0.710	-0.174	0.373	0.758	0.801	0.710	0.717	0.660	0.965	0.895	0.884	0.872
6 (FW1-SR)	slope	-0.301	-0.080	1.781	5.773	0.823	0.328	2.837	1.009	4.084	3.374	0.419	0.212
	y intercept	18.0	15.9	128.7	119.4	23.6	27.1	146.0	47.3	97.6	110.0	9.5	12.9
	corr coeff	-0.696	-0.256	0.388	0.753	0.847	0.555	0.621	0.663	0.934	0.843	0.889	0.743
7 (FW3-SR)	slope	0.293	0.602	0.619	0.330	2.032	2.446	2.281	1.812	1.186	2.068	1.217	0.912
	y intercept	82.2	75.5	92.7	97.4	78.7	88.1	108.7	107.4	85.5	81.7	29.4	37.7
	corr coeff	0.193	0.590	0.469	0.279	0.916	0.832	0.769	0.580	0.734	0.851	0.928	0.928
8 (FW3-FW1)	slope	-0.631	-0.163	0.777	2.239	1.035	0.614	3.355	0.973	3.501	2.835	0.579	0.479
	y intercept	50.7	46.5	49.8	40.5	36.9	41.7	168.6	60.4	116.8	119.2	14.8	19.1
	corr coeff	-0.638	-0.202	0.436	0.754	0.856	0.791	0.705	0.580	0.908	0.839	0.908	0.889

APPENDIX B

INSTRUMENTATION

This section briefly describes the instruments used in the fatigue muscle studies for the two on going research projects at Kessler Institute for Rehabilitation.

1. SURFACE ELECTRODES:

This electrode was used to pick up EMG available from the surface of the skin. The two types of surface electrode used were the following

- a. Delsys™ surface EMG differential electrode and
- b. Teca™ bipolar surface bar electrode.

A. Delsys Electrode (#DE02):

This is surface EMG differential electrode having high input impedance, balanced, stable differential amplifier with a gain of approximately 10. The detection surfaces consists of two parallel silver bars, each 1.0 cm long and 1.0 cm wide, space 1.0 cm apart.

This electrode does not require any special skin preparation. The electrode can be attached with adhesive tape. Figure B.1 shows this type of electrode.

B. Teca Electrode (#922-603-1):

This is a surface EMG bipolar passive stainless steel bar electrode. The inter electrode distance is 3.0 cm. This electrode requires special skin preparation for effective function.

It is recommended to remove the dead surface layer of the skin along with protective hair to lower the electrical impedance. This electrode requires gel for effective skin-electrode contact.

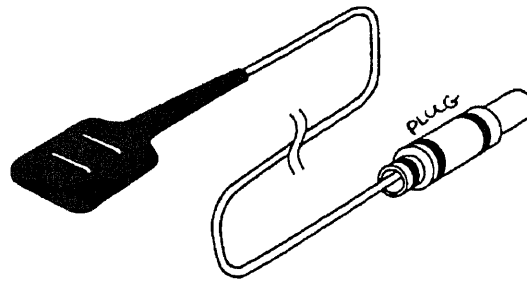


Figure B.1 shows Delsys™ electrode.

2. FINE WIRE ELECTRODE

The fine wire electrode is used to record the EMG signal from deep muscles. The fine wire electrode used for group II was 20 μm stainless steel wire coated with Teflon which acts as insulation. This fine wire is assembled in a stainless steel 27-gauge needle.

3. ISOLATION PRE AMPLIFIER (Gould # 11-5407-58)

This amplifier provides the required signal isolation between the subject and the measuring equipment. The unit can be placed near the signal source. The pre amplifier conditioned the signal before being degraded by noise pickup or the capacitance of long signal cables. This amplifier has a gain of 20 and input impedance >1000 mohms. Figure B.2 show this amplifier.

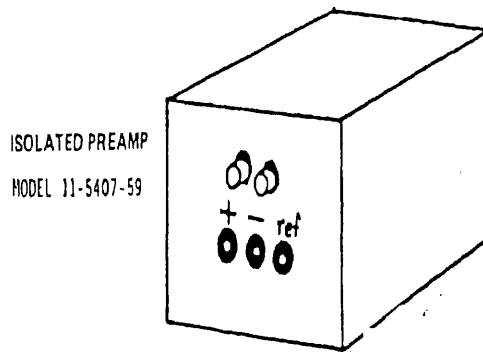


FIGURE B.2 shows the isolation pre amplifier

4. UNIVERSAL AMPLIFIER (Gould # 13-4615-58)

This amplifier acted as an excellent differential signal conditioner, having high input impedance, wide bandwidth, low noise. This amplifier served as a biophysiological amplifier along with the isolation amplifier.

This amplifier has measurement range

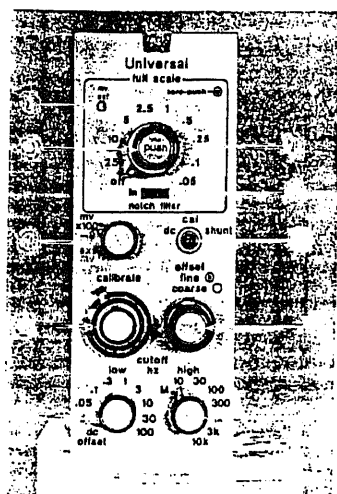
“mv X 100” 2.5 mV full scale to 10 V full scale.

“mv” or “ext mv” 25 μ V scale to 250 mV full scale.

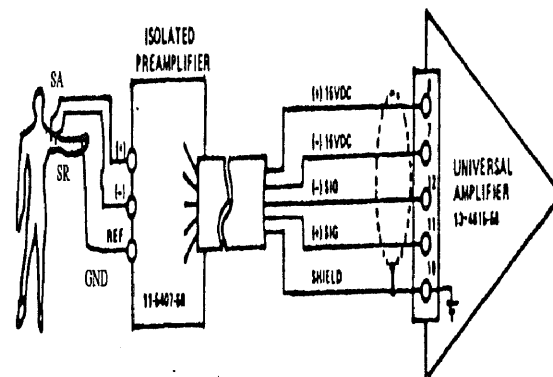
Attenuation.....0.05, 0.1, 0.25, 0.5, 1, 2.5, 5, 10, 25, full scale and off, “mvX100/mv/ext mv” switch and “calibrate” vernier dial

Calibrated Vernier.....10 turn vernier to multiply setting of attenuator.

input impedance 100 megohm. Figure B.3 A shows universal amplifier and B shows isolated preamp connections.



A



B

Figure B.3 A. Gould Universal Amplifier (13-4615-58); B. Isolated Preamp connections.

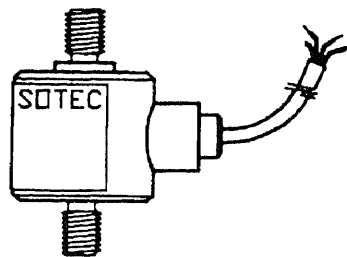
5 DATA ACQUISITION BOARD (Kiethley MetraByte #DAS1601)

This is a high speed A/D interface board for the IBM PC and its compatibles. The board installs directly into a computer slot. It can handle samples upto 100ks/sec. It has 16 single ended or 8 differential analog input channels. It also supports software STREAMER which is a menu-driven data acquisition software for high speed transfer of DAS-16 data directly to the hard disk.

6. HAND HELD DYNAMOMETER:

This is an instrument used to measure force produced during isometric contraction. This unit was assembled in-house in our research lab. The force was sensed using a precision miniature SENSOTEC's load cell model 31. This load cell utilizes high quality strain gage, precision gaging techniques and welded stainless steel construction to provide

precise, reliable force measurement. This tension/compression load cell has male threads to which is attached mounting studs that attaches to a physiotherapist adapter. This adapter is concave shaped and acts as an interface between the muscle under test and the transducer. The load cell is excited by the GM unit which has a 10 v transducer excitation supply, an amplified 0-5V DC output, a 4 1/2 digit display and a shunt calibration on the front panel. Figure B.4 shows SENSOTECH's model 31 Load cell.



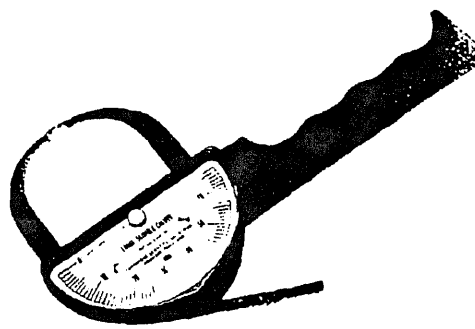
**Model 31 Male Threads
(Tension/Compression)**

Figure B.4 Sensotech's Load cell.

7. SKIN FOLD CALIPER: (Lange #HB859-12)

This is a precision instrument designed to make accurate measurement of subcutaneous tissue. It has a pivoted tip which adjust automatically for parallel measurements of skin fold. It has rectangular faces with well rounded edges at the corners which assures subject comfort.

As one half of body fat is located directly beneath the skin, total body fat can be computed by making skinfold measurements. To make accurate measurements it is recommended to take skin fold measurement directly under the skin and not through the clothing. The skinfold was measured by picking up and holding the skin fold with one hand, while measuring the skinfold with the caliper held by the other hand. Three measurements are made and the average of three measurements is that of the skinfold. Figure B.5 A shows the Lange™ skinfold caliper; and B during its use.



LANGE SKINFOLD CALIPER...

A



B

Figure B.5 A Lange skinfold caliper; B Caliper in use.

APPENDIX C

Data Acquisition

1. Protocol for The Data Acquisition for Group I

As described in the section 2.3 the data was acquired using an analog to digital conversion interface board (Kiethley MetraByte #DAS1601) and the data acquisition software (Kiethley MetraByte #STREAMER V3.5). But, before acquiring data it was required to create files of appropriate size for data storage. This operation of creating file was performed using STREAMER'S MKFILE command. The command required to give the name of the file and the size of the file into terms of kilobytes (KB).

The size of file was calculated using the sampling rate (S) per channel, the number of channels to be acquired (C), and the total sampling time (T).

$$size = S \times C \times T \times 2 \quad (\text{KB}) \quad (\text{C.1})$$

The sampling rate (S) chosen for this project was 2000 Hz as the highest frequency was estimated to be 1000 Hz. The duration (T) of each experiment was 45 sec and number of channels acquired (C) were 2, one was from EMG picked up by the surface electrode and other was the force output from the SENSOTEC. Now substituting all this values in the formula (C.1) gives the file of the required file size.

$$size = 2000 \times 2 \times 45 \times 2 = 360 \quad (\text{KB}) \quad (\text{C.2})$$

Due to limitation in the unpack utility, each data file was unpacked into 2 files and was later joined together before processing using program written in MATLAB (See

Appendix D for programming details). A batch file, 2file.bat, was used to unpack 2 files at one time and contained the code as follows:

```
kunpack2 1.dat,%1.1,0-89999/b/das16
kunpack2 1.dat,45000-179999/b/das16.
```

An example of execution of this operation on a file at the system prompt using this batch file is:

```
2file r120894a
```

results in

```
kunpack2 r120894a.dat,r120894a.1,0-89999/b/das16
kunpack2 r120894a.dat,r120894a.2,90000-179999/b/das16.
```

2. Protocol for Data Acquisition for Group II

The data acquisition board and the data acquisition software were the same as Group I. The size of file was calculated using formula C.1. The sampling rate chosen for this project was 3000 Hz as the highest frequency component in the signal was estimated to be 1500 Hz. The duration (T) of each trial was 30 sec and number of channels acquired (C) were 8, formed as a result of different combinations of fine wire and surface electrodes as described in the section 2.2.1. Therefore substituting the above parameters in the equation C.1 yields

$$size = 3000 \times 8 \times 30 \times 2 = 1440 \text{ (KB)} \quad (C.3)$$

Due to limitations in the unpack utility for handling large samples of data and large memory requirements in Matlab, each data file was unpacked into 15 files of 2 seconds each at one time using a batch file, 15file.bat, and contained the code as follows:

```
kunpack2 %1.dat,%1.1,0-47999/b/das16
kunpack2 %1.dat,%1.2,48000-95999/b/das16
.
.
.
.
kunpack %1.dat,%1.15,672000-719999/b/das16.
```

An example of execution of this operation on a file at the DOS (disk operating system)

prompt using this batch file is:

```
15file djr1218a
```

results in

```
kunpack2 djr1218a.dat,djr1218a.1,0-47999/b/das16
.
.
.
.
kunpack2 djr1218a.dat,djr1218a.15,672000-719999/b/das16.
```

APPENDIX D

FLOW CHART AND PROGRAMMING DETAILS

1. Flow Chart and Programming Details for Group I

This section describes about the software tool developed in MATLAB language for this group. In this project as discussed in section 1 of Appendix C, a 45 sec file was divided into 2 files and before processing was joined together using the following program.

INP.M

```
clear f_name
f_name=input('Please enter the name of file to be loaded->','s');
file=[];
for i=1:1:2
    f_str=sprintf('%s.%s',f_name,num2str(i));
    eval(['load ' f_str]);
    file=[file
    eval(f_name)];
end
eval(['clear ' f_name]);
```

The merged files was then processed for estimation of median frequency and these median frequency points in turn were processed for linear regression calculation and sent for plotting as illustrated in the flow chart and the source code as shown below.

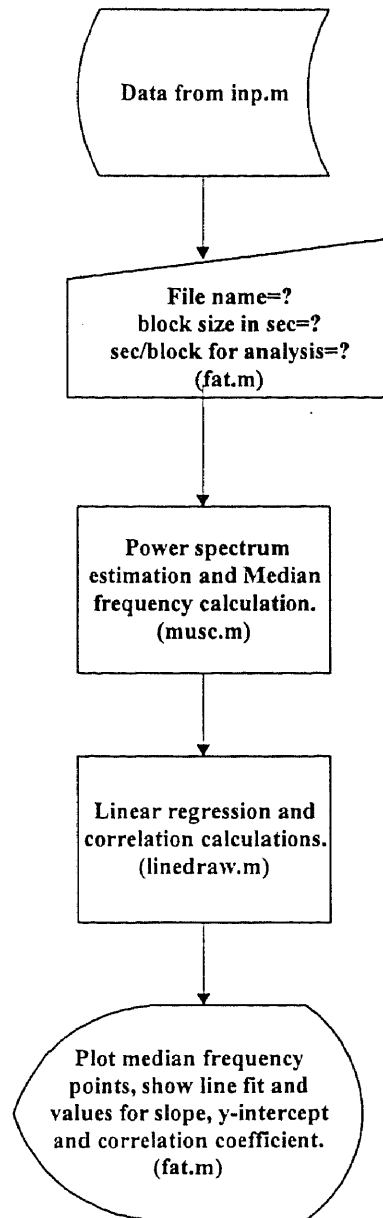


Figure D.1 shows the Flow chart of the software tool developed for group I.

FAT.M

This subroutine is the main routine of the entire source code of this project. This program calls several other subroutine (functions) and plots the required results.

clc

```

disp('          WELCOME          ');
disp(' TO THE WORLD OF SIGNAL PROCESSING  ');
disp(' AT Kessler Institute for Rehabilitation ');

disp('    Developed by          Rakesh Maniar          ');
disp('    Thanks to          John Andrews          ');

ana_file=input('Please enter the name of the file without extension--> ','s');
secperblock=input('Please enter #seconds per analysis block :-->');
interestsec=input('Enter the total number of seconds data for analysis:--> ');
tic;
SampleRate=2000;                                %sampling rate is 2000 for this group.
originallengthsec=45;                            %Duration of the experiment.
originarraylength=originallengthsec*SampleRate;  %number of samples to read in
interestarraylength=interestsec*SampleRate;     %num samples to use for analysis

finalmedianarray=[]; finalmedianpoints=[];
MedianFreqDArray=[];
loadfile=sprintf('%s.asc',ana_file);

disp(sprintf('Accepting first %d data points (%d seconds) as data of
Interest...!',interestarraylength,interestsec))
disp(sprintf('Rejecting %d seconds of data from each block...!',secperblock-interestsec));
disp(sprintf('Rejecting first %d seconds (1 block) of data...!',secperblock));
DMatrix=[];

no_of_blocks=fix(originallengthsec/secperblock);
DMatrix=file(1:originarraylength,ch);
blocksize=length(DMatrix)/no_of_blocks;

for Block=2:1:no_of_blocks,
    disp(sprintf('*****%d**',Block))
    TempArray=DMatrix((Block-1)*blocksize+1:(Block*blocksize));
    FinArray=TempArray(1:interestarraylength);
    MedianFreqDPoint=musc(FinArray,SampleRate);
    clear TempArray FinArray;
    MedianFreqDArray=[MedianFreqDArray MedianFreqDPoint];
end

    finalmedianarray=MedianFreqDArray;

end

%determine least-squares fit and plotting result

```

```

for i=1:1:1
    VarY=linedraw(finalmedianarray,sprintf('%s.%s',ana_file,num2str(i)), ...
    secerblock);                                %least squares fit routine
end

%Generate plots of raw dat

%scale to Sec for plotting
t=1:10:length(DMatrix);
taxis=t/SampleRate;

figure
subplot(2,1,1)
plot(taxis,file(t,1),'r')
V=axis;
grid
title(sprintf('%s raw data report',ana_file))
xlabel('Amplitude vs. Sec')
subplot(2,1,2)
[b,a]=butter(1,.00025);                        %processing force channel
filt_force=filter(b,a,file(:,2));             %using low pass filter at cut off at 0.5 Hz.
plot(taxis,filt_force(t)/4.125,'c')
grid
ylabel('Force lbs')
xlabel('Sec')
title('Force maintained at 50% Maximal Voluntary Contraction')
toc

```

MUSC.M

```

function medfreq=musc(x,Fs);

% Determines median frequency trend from array of EMG data

% lowerfreq is lower frequency for plotting spectrum
% upperfreq is higher frequency freq for plotting spectrum
% timelength is number of seconds of data to run
% fftsize is size of fft to calculate
% Fs is sampling rate of the signal

lowerfreq=30;
upperfreq=512;

```



```

% prevent a 0 in lower frequency
if lowerfreq<=0,lowerfreq=.2;, end

%take FFT

clear y w
fftsize=length(x);
low=fftsize*lowerfreq/Fs;
high=fftsize*upperfreq/Fs;

    %put alternative fft method here
x=x-mean(x);
fftx=fft(x,fftsize);
Pyy=fftx.*conj(fftx)/fftsize;
f=Fs*(0:(fftsize/2-1))/fftsize;
clear fftx w x y

    % calculate median frequency
i=low-1;
ampsum=0;
desired=sum(Pyy(low:high))/2; %taking data between frequencies
while ampsum < desired
    i=i+1;
    ampsum=Pyy(i) + ampsum;
end
medfreq=f(i);

```

LINEDRAW.M

```

function P=linedraw(x,plotfitfilename,SecondsPerBlock)

% linedraw.m
% Creates a new vector based on linear regression and plots data with best-fit line, slope,
intercept, and correlation coefficient.
% USES data in workspace: x
% USES data in workspace: plotfitfilename
% CREATES 1x3 vector P=[slope, intercept,coeff]
% CALLS Function LineFit for regression calculations
%
last=length(x)
P=linefit(x(1:last))
newx=1:1:last-1;

```

```

newpfity=P(2)+P(1).*newx;
figure
plot(x(1:last),'c*')
hold
plot(newpfity,'r')
hold off
tstring1=sprintf('slope = %4.3f,P(1));
tstring2=sprintf('y int = %4.3f,P(2));
tstring3=sprintf('r val = %1.3f,P(3));
text(6,min(x(2:last))+1.*(max(x(2:last))-min(x(2:last))),tstring1)
text(6,min(x(2:last))+.95*(max(x(2:last))-min(x(2:last))),tstring2)
text(6,min(x(2:last))+.90*(max(x(2:last))-min(x(2:last))),tstring3)

title(sprintf('%s sequential %d sec. intervals',plotfitfilename,SecondsPerBlock))
xlabel(' Interval Number')
ylabel('Median Frequency over 30-512Hz')

clear newx newpfity tstring1 tstring2 tstring3 P

```

LINEFIT.M

```

%Function Linefit.m
function lineFit=fit(y)
% Determine coefficients of a least-squares fit to
% data vector passed in y, storing parameters in
% 1x3 vector P[ slope intercept coeff]

% USES data passed in y
% CREATES 1x3 vector P=[slope, intercept, coeff]

x=1:length(y);
Mnum=sum(x.*y)-sum(x)*sum(y)/length(x);
den=sum(x.*x)-sum(x)^2/length(x);
Mslope=Mnum/den
%Bintercept
Bnum=[sum(x.*x)*sum(y)-sum(x)*sum(x.*y)]/length(x);
Bintercept=Bnum/den;
rcoeff=Mnum/sqrt(den*[sum(y.*y)-sum(y)^2/length(x)]);
lineFit=[ Mslope Bintercept rcoeff];

```

This is basically user friendly program wherein the user has to enter few information it asks for and has to wait for only 15 sec to process a file. The gist of this program is that it has been written in batch mode and it automatically picks n sec of data (2 secs for this project) process it and again load another n sec till end of data is reached.

2. Flow Chart and Programming Details for Group II

This section describes about the program developed in MATLAB language for this group. As discussed in the section 2.6 it was required to estimate median frequency, mean frequency and root means square for all the 8 channels contained in each of the 15 two sec files. The entire processing of data has been illustrated in the flow chart. The source code written to achieve this goal has been provided below.

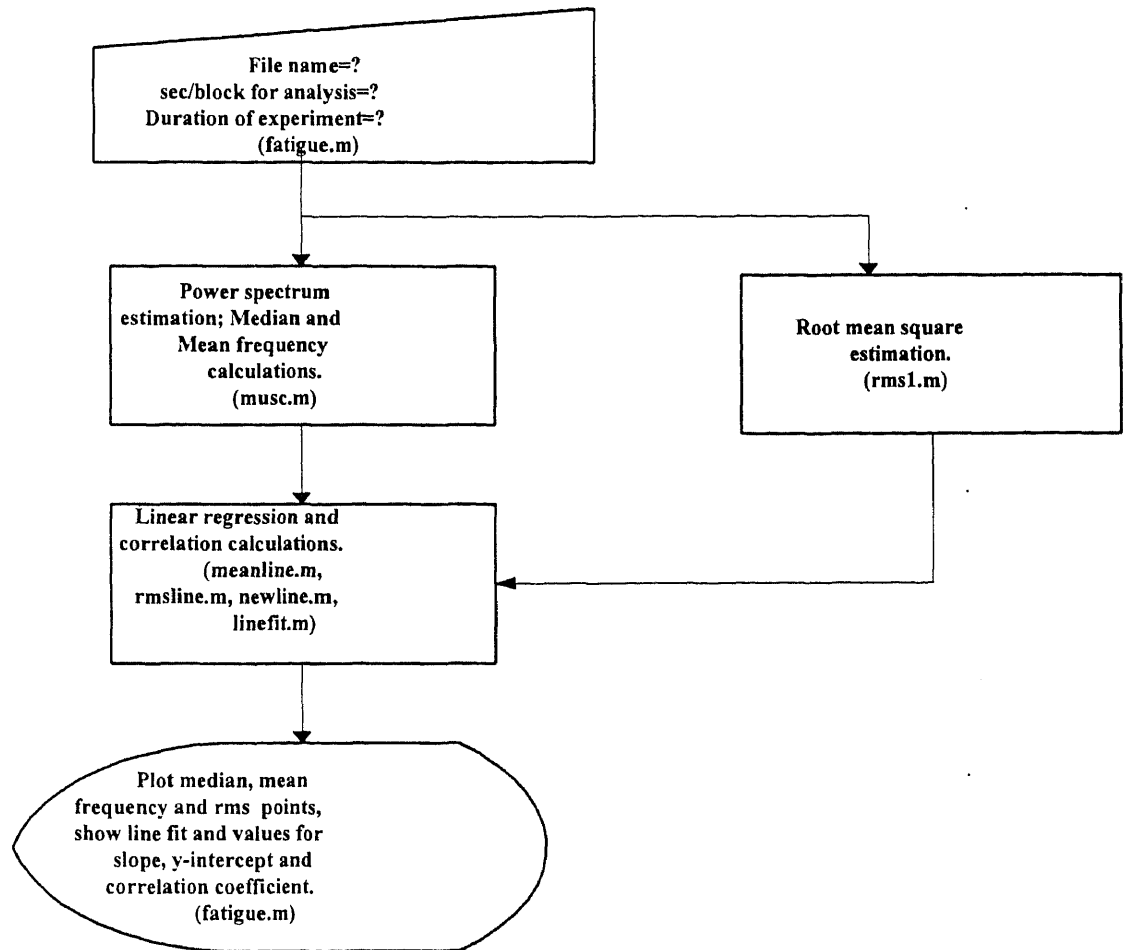


Figure D.2 shows the flow chart of the software developed for Group II

FATIGUE.M

```

clc
disp('          WELCOME          ');
disp('TO THE WORLD OF SIGNAL PROCESSING ');
disp(' AT Kessler Institute for Rehabilitation ');

disp('   Developed by       Rakesh Maniar   ')

filestr=input('Enter the name of the file without extension-->','s');
  
```

```

interestsec=input('Please enter #seconds per analysis block:-->');
totalsec=input('Please enter the total seconds of experiment:-->');
samplerate=3000;
unpacksec=2;
tic
originarraylength=unpacksec*samplerate;
interestarraylength=interestsec*samplerate;

numoffiles=ceil(totalsec/unpacksec);
finalmedianarray=[]; finalrmsarray=[]; finalmeanarray=[];
finalmedianpoints=[];finalrmspoints=[]; finalrmspoints=[];
for f = 2:1:numoffiles,
    disp(sprintf('*****%d*****',f))
    filename=sprintf('%s.%s',filestr,num2str(f));
    eval(['load ' filename]);
    file=eval(filestr);    % file loaded

    for ch =1:1:8,
        disp(sprintf('*****%d.%d*',f,ch))
        file_ch=file(1:interestarraylength,ch);
        len=length(file_ch);
        [medianpoint meanpoint]=mus(file_ch(1:len),samplerate);
        rmspoint=rms1(file_ch(1:len));
        medianarray=( [medianarray medianpoint] );
        meanarray=( [meanarray meanpoint] );
        rmsarray=( [rmsarray rmspoint] );

    end
    finalmedianpoints=( [finalmedianpoints medianarray] );
    finalmeanpoints=( [finalmeanpoints meanarray] );
    finalrmspoints=( [finalrmspoints rmsarray] );

    medianarray=[]; rmsarray=[]; meanarray=[];
end
[m1 m2 m3 m4 m5 m6 m7 m8]=separate(finalmedianpoints,ch);
[r1 r2 r3 r4 r5 r6 r7 r8 ]=separate(finalrmspoints,ch);
[q1 q2 q3 q4 q5 q6 q7 q8 ]=separate(finalmeanpoints,ch);
finalmedianarray=[finalmedianarray; m1' m2' m3' m4' m5' m6' m7' m8' ];
finalmeanarray=[finalmeanarray; q1' q2' q3' q4' q5' q6' q7' q8'];
finalrmsarray=[finalrmsarray; r1' r2' r3' r4' r5' r6' r7' r8'];
clear r1 r2 r3 r4 r5 r6 r7 r8 m1 m2 m3 m4 m5 m6 m7 m8
clear q1 q2 q3 q4 q5 q6 q7 q8

% least square fit and generating result

```

```

savemed=sprintf('%s.m',filestr);           %save mean, median frequency and rms
saverms=sprintf('%s.r',filestr);          %point
savemea=sprintf('%s.n',filestr);

eval(['save ' savemed ' finalmedianarray -ascii']);
eval(['save ' saverms ' finalrmsarray -ascii']);
eval(['save ' savemea ' finalmeanarray -ascii']);

for I =1:1:8,
    newline(finalmedianarray(:,I),sprintf('%s.%s',filestr,num2str(I)),interestsec);
    meanline(finalmeanarray(:,I),sprintf('%s.%s',filestr,num2str(I)),interestsec);
    rmsline(finalrmsarray(:,I),sprintf('%s.%s',filestr,num2str(I)),interestsec);
end
toc

```

MUS.M

```

function [medfreq, meanfreq] =mus(x,Fs);

% Determines median frequency trend from array of EMG data
%   lowerfreq is lower freq for plotting spectrum
%   upperfreq is upper freq for plotting spectrum
%   timelength is number of seconds of data to run
%   fftsize is size of fft to calculate
%   Fs is sampling rate of the signal

    lowerfreq=30;
    upperfreq=1000;

% prevent a 0 in lower frequency
    if lowerfreq<=0,lowerfreq=.2;, end

%take FFT
    fftsize=length(x);
    low=fftsize*lowerfreq/Fs;
    high=fftsize*upperfreq/Fs;

%put alternative fft method here
    x=x-mean(x);
    fftx=fft(x,fftsize);
    Pyy=fftx.*conj(fftx)/fftsize;
    f=Fs*(0:(fftsize/2-1))/fftsize;
    clear fftx

```

```

% calculate median frequency
i=low-1;
ampsum=0;
desired=sum(Pyy(low:high))/2; %taking data between frequencies
while ampsum < desired
    i=i+1;
    ampsum=Pyy(i) + ampsum;
end
medfreq=f(i);

```

```

% calculate mean frequency
j=low:high;
Py=Pyy';
meanfreq=sum((Py(j).*f(j)))/(sum(Py(low:high)));

```

RMS1.M

%Computes RMS value of array of data

```

function y = rms1(x);
m_x=x-mean(x); %remove dc level
rect_m_x=sqrt(m_x.^2);
y=sqrt(mean(rect_m_x.^2));

```

SEPARATE.M

%This separates datafile into 8 channels

```

[a, b, c, d, e,f,g,h] =separate(datafile,ch);
tempx=[];
tempx=datafile;
j=1:1:length(tempx)/ch;
n=1:ch:length(tempx);
a(j)= tempx(n); %first channel data
b(j)=tempx(n+1); %second channel data
c(j)=tempx(n+2); %third channel data
d(j)=tempx(n+3); %fourth channel data
e(j)=tempx(n+4); %fifth channel data
f(j)=tempx(n+5); %sixth channel data

```

```

g(j)=tempx(n+6);    %seventh channel data
h(j)=tempx(n+7);    %eighth channel data

```

NEWLINE.M

```

function P=newline(x,plotfitfilename,SecondsPerBlock)

% Creates a new vector based on linear regression
% and plots data with best-fit line, slope, intercept,
% and correlation coefficient.
% USES data in workspace: x
% USES data in workspace: plotfitfilename
% CREATES 1x3 vector P=[slope, intercept,coeff]
% CALLS Function LineFit for regression calculations
%
last=length(x)
P=linefit(x(1:last))
newx=1:1:last;
newpfity=P(2)+P(1).*newx;
figure
plot(x(1:last),'w*')
hold
plot(newpfity,'r')
hold off
tstring1=sprintf('slope = %4.3f,P(1));
tstring2=sprintf('y int = %4.3f,P(2));
tstring3=sprintf('r val = %1.3f,P(3));
text(7,min(x(1:last))+1.*(max(x(1:last))-min(x(1:last))),tstring1)
text(7,min(x(1:last))+.95*(max(x(1:last))-min(x(1:last))),tstring2)
text(7,min(x(1:last))+.90*(max(x(1:last))-min(x(1:last))),tstring3)
title(sprintf('%s sequential %d sec. intervals',plotfitfilename,SecondsPerBlock))
xlabel(' interval number')
ylabel('Median Frequency over 30-1000Hz')
clear newx newpfity tstring1 tstring2 tstring3 P

```

MEANLINE.M

```

function Q=meanline(x,plotfitfilename,SecondsPerBlock)

% Creates a new vector based on linear regression
% and plots data with best-fit line, slope, intercept,

```



```

% and correlation coefficient.
% USES data in workspace: x
% USES data in workspace: plotfitfilename
% CREATES 1x3 vector P=[slope, intercept,coeff]
% CALLS Function LineFit for regression calculations

last=length(x)
P=linefit(x(1:last))
newx=1:1:last;
newpfity=P(2)+P(1).*newx;
figure
plot(x(1:last),'w*')
hold
plot(newpfity,'r')
hold off
tstring1=sprintf('slope = %4.3f,P(1));
tstring2=sprintf('y int = %4.3f,P(2));
tstring3=sprintf('r val = %1.3f,P(3));
text(10,min(x(1:last))+1.*(max(x(1:last))-min(x(1:last))),tstring1)
text(10,min(x(1:last))+.95*(max(x(1:last))-min(x(1:last))),tstring2)
text(10,min(x(1:last))+.90*(max(x(1:last))-min(x(1:last))),tstring3)

title(sprintf('%s sequential %d sec. intervals',plotfitfilename,SecondsPerBlock))
xlabel(' interval number')
ylabel('Mean Frequency over 30-1000Hz')
clear newx newpfity tstring1 tstring2 tstring3 P

```

RMSLINE.M

```

function P=rmsline(x,plotfitfilename,SecondsPerBlock)

% Creates a new vector based on linear regression
% and plots data with best-fit line, slope, intercept,
% and correlation coefficient.
% USES data in workspace: x
% USES data in workspace: plotfitfilename
% CREATES 1x3 vector P=[slope, intercept,coeff]
% CALLS Function LineFit for regression calculations

last=length(x)
P=linefit(x(1:last))
newx=1:1:last;
newpfity=P(2)+P(1).*newx;

```

```

figure
plot(newx,x(1:last),'w+',newx,x(1:last),'g-')
hold
plot(newpfity,'r')
hold off
tstring1=sprintf('slope = %4.3f,P(1));
tstring2=sprintf('y int = %4.3f,P(2));
tstring3=sprintf('r val = %1.3f,P(3));
text(10,min(x(1:last))+1.*(max(x(1:last))-min(x(1:last))),tstring1)
text(10,min(x(1:last))+.95*(max(x(1:last))-min(x(1:last))),tstring2)
text(10,min(x(1:last))+.90*(max(x(1:last))-min(x(1:last))),tstring3)

title(sprintf('%s sequential %d sec. intervals',plotfitfilename,SecondsPerBlock))
xlabel(' interval number')
ylabel('Root Mean Square ')
clear newx newpfity tstring1 tstring2 tstring3 P

```

LINEFIT.M

```

function lineFit=fit(y)
% Determine coefficients of a least-squares fit to
% data vector passed in y, storing parameters in
% 1x3 vector P[ slope intercept coeff]
% USES data passed in y
% CREATES 1x3 vector P=[slope, intercept, coeff]

x=1:1:length(y);
Mnum=sum(x.*y)-sum(x)*sum(y)/length(x);
den=sum(x.*x)-sum(x)^2/length(x);
Mslope=Mnum/den
%Bintercept
Bnum=[sum(x.*x)*sum(y)-sum(x)*sum(x.*y)]/length(x);
Bintercept=Bnum/den;
rcoeff=Mnum/sqrt(den*[sum(y.*y)-sum(y)^2/length(x)]);
lineFit=[ Mslope Bintercept rcoeff];

```

This is also very user friendly program. This program assumes that 15 files of 2 sec each is available in the working directory. While processing the file it gives visual display to user as to which file and which channel in that file it is processing. The processing time for one entire 30 sec file is approximately 3 minutes.

APPENDIX E

POWER ANALYSIS

Power analysis is a tool for estimating the number of subjects required to detect both clinically and statistically the differences between the two groups. In order to perform power analysis, the following specifications are required:

- a. Null hypothesis and one or two tailed alternative hypothesis.
- b. Alpha (α) level.
- c. Beta (β) level and
- d. Effect size.

The number of subjects needed in a study can be decreased by increasing alpha, beta or the effect size [25].

Discussing each of these specifications very briefly, the purpose of hypothesis testing is to aid clinicians, researchers, or administrators in reaching a decision concerning a population by examining a sample from that population. A hypothesis may be defined simply as a statement about one or more populations.[10]. There are essentially two statistical hypotheses: Null hypothesis, also referred to as a hypothesis of no differences between two groups, and an alternative hypothesis, the hypothesis that disproves the null hypothesis. If both large and small values of test statistics will cause rejection of the null hypothesis, this is called two sided hypothesis testing and if either

sufficiently small values only or sufficiently large values only will cause rejection of the null hypothesis; one sided hypothesis is said to be tested.

The alpha level is the probability of rejecting a true null hypothesis. Since rejecting a true null hypothesis will constitute an error, it becomes reasonable to make the alpha as small as possible. The most frequently used values for alpha are 0.01, 0.05, and 0.10. [10]. The error committed when a true null hypothesis is rejected is called a type I error. The beta level is the error (type II) committed when a false null hypothesis is accepted. The probability of committing a type II error is designated by β . The effect size is the amount of difference between groups one wants to be able to detect.

Let us discuss the power analysis techniques used for the two ongoing research projects at the Kessler Institute for Rehabilitation designated as group I and group II .

1. Power Analysis for Group I:

This study establishing normal values for the median frequency and its slope with fatigue is a descriptive study as the variable of interest (the range of median frequency) is a continuous variable. To establish the sample size, the following steps are to be performed:

- a. Estimation of the standard deviation of the variable of interest.
- b. Specification of the desired precision (total width) of the interval.
- c. Selection of the confidence level.

Table E.1 is then used to determine the number of subjects required to validate the results.

We performed the above steps using the following values:

a standard deviation of 8 Hz (based on previous study[11]); total width of confidence interval of 4 Hz, giving the standardized width of the confidence interval (computed as total width divided by standard deviation) of 0.5; and chosen confidence level of 95%.

Referring to table E.1 and reading across from a standardized width of 0.5 in the leftmost column and down from the 95% confidence level, the required sample size is **62** subjects.

Table E.1 Sample size for common values of W/S.

W/S	Confidence Level		
	90 %	95 %	99 %
0.10	1083	1537	2665
0.15	482	683	1180
0.20	271	385	664
0.25	174	246	425
0.30	121	171	295
0.35	89	126	217
0.40	68	97	166
0.50	44	62	107
0.60	31	43	74
0.70	23	32	55
0.80	17	25	42
0.90	14	19	33
1.00	11	16	27

Source: S. B. Hulley and S. R. Cummings, "Sample size for a descriptive study for a continuous variable," Designing Clinical Research. (Philadelphia: Williams & Wilkins) 219.

2. Power Analysis for Group II

The power analysis of this group concerning different electrode types and placement was based on ability to detect a correlation coefficient of 0.5 or better, with β of 0.2 and with a two tailed α of 0.05; and referring to table E.2 reading across from the correlation coefficient (r) of 0.5 in the leftmost column and down from the two-tailed α of 0.05 and β of 0.2 shows **29** subjects are needed to validate results.

Table E.2 Sample size for revealing a correlation.

r^*	One-tailed $\alpha =$	0.005			0.025			0.05		
	Two-tailed $\alpha =$	0.01			0.05			0.010		
	$\beta =$	0.05	0.10	0.20	0.05	0.10	0.20	0.05	0.10	0.20
0.05		7118	5947	4663	5193	4200	3134	4325	3424	2469
0.10		1773	1481	1162	1294	1047	782	1078	854	616
0.15		783	655	514	572	463	346	477	378	273
0.20		436	365	287	319	259	194	266	211	153
0.25		276	231	182	202	164	123	169	134	98
0.30		189	158	125	139	113	85	116	92	67
0.35		136	114	90	100	82	62	84	67	49
0.40		102	86	68	75	62	47	63	51	37
0.45		79	66	53	58	48	36	49	39	29
0.50		62	52	42	46	38	29	39	31	23
0.60		40	34	27	30	25	19	26	21	16
0.70		27	23	19	20	17	13	17	14	11
0.80		18	15	13	14	12	9	12	10	8

Source: S. B. Hulley and S. R. Cummings, "Total sample size required when using the correlation coefficient," *Designing Clinical Research*. (Philadelphia: Williams & Wilkins) 218.

REFERENCES

1. Basmajian, J.V. and C.J. De Luca. *Muscles Alive*. 5th edition., Baltimore, Williams and Wilkins Publishers (1985).
2. Bendat, J. and A. Piersol. *Measurement and Analysis of Random Data*. New York, Wiley (1966).
3. Bilodeau, M., A.B. Arsenault, D. Gravel, D. Bourbonnais, and F. Kemp. "The Influence of Gender on the EMG Power Spectrum of Elbow Flexors and Extensors." *IEEE Engineering in Medicine and Biology Society*. 13(2), (1991): 841-842.
4. Bohannon, R.W. "Comparability of Force Measurements Obtained with Different Strain Gauge Hand-Held Dynamometer." *J. Orthop Sports Phys Ther*. 18(4), (1993): 564-567.
5. Brody, L.R., M.T. Pollock, S.H. Roy, C.J. Deluca, and B. Celli. "PH-Induced Effects on Median Frequency and Conduction Velocity of the Myoelectric Signal." *J. Appl Physiol*. 71(5), (1991): 1878-1885.
6. Broman, H., G. Bilotto, and C.J. De Luca. "Myoelectric Signal Conduction Velocity and Spectral Parameters: Influence of Force and Time." *J. Appl Physiol*. 58(5), (1985): 1428-1437.
7. Chaffin, D.B. "Localized Muscle Fatigue- Definition and Measurement." *J Occup Med*. 15, (1973): 346-354.
8. Cromwell, L., F.J. Weibell, and E.A. Pfeiffer. *Biomedical Instrumentation and Measurements*, 2nd edition., New Delhi, Prentice-Hall of India., (1990).
9. Daanen, H.A., M. Mazure, M. Holewijn, and E.A. Van der Velde. "Reproducibility of the Mean Power Frequency of the Surface Electromyogram." *Eur. J. Appl Physiol*. 61(3-4), (1990): 274-277.
10. Daniel, W. W. *Biostatistics: A Foundation for Analysis in the Health Sciences*. 5th edition., New York, John Wiley & Sons (1991).
11. Davies, M. R. "Time Frequency Analysis of Electromyogram During Muscle Fatigue." *MS Thesis*, New Jersey Institute of Technology, January 1994.

12. De Luca, C.J., M.A. Sabbahi, F.B. Stulen, and G. Brilotto. "Some Properties of the Median Frequency of the Myoelectric Signal during Localized Muscular Fatigue." *Proc. of the 5th Internat. Sym. on the Biochemistry of Exer., Human Kinetics Publishers, Chicago, IL* (1983): 175-186
13. Delagi, E.F., A. Perotto, J. Iazzetti and D. Morrison. *Anatomical Guide for the Electromyographer: The Limbs and Trunks*. 3rd edition, Springfield, Charles C Thomas Publishers (1990).
14. Duchateau, J. and K. Hainaut. "Effects of Immobilizations on Electromyogram Power Spectrum Changes During Fatigue." *Eur. J. Appl Physiol.* 63, (1991): 458-462.
15. Duchene, J., and F. Gouble. "EMG Spectral Shift as an Indicator of Fatigability in an Heterogeneous Muscle Group." *Eur. J. Appl Physiol.* 61(1-2), (1990): 81-87.
16. Durnin, J.V.G.A and J. Womersley. "Body Fat Assessed from Total Body Density and its Estimation From Skin-Fold Thickness: Measurements on 481 Men and Women Aged from 16 to 72 Years." *Br. J. Nutr.* 32, (1974): 77-97.
17. Gerdle, B., N.E. Eriksson, and L. Brundin. "The Behaviour of the Mean Power Frequency of the Surface Electromyogram in Biceps Brachii with Increasing Force and During Fatigue. With Special Regard to the Electrode Distance." *Electromyogr. Clin. Neurophysiol.* 30, (1990): 483-489.
18. Getchell, B. *Physical Fitness-A Way of Life*, 2nd edition., New York, John Wiley & sons (1979).
19. Guyton, A.C. *Textbook of Medical Physiology*, 8th edition., Philadelphia, W.B. Saunders Company., (1991).
20. Hagg, G.M. "Comparison of Different Estimators of Electromyographic Spectral Shifts during work When Applied on Short Test Contractions." *Med Bio Eng Comput.* 29(5), (1991): 511-516.
21. Hulley, S. B and S. R. Cummings. *Designing Clinical Research*. Philadelphia, Williams & Wilkins.
22. Johnson, M.A., J. Polgar, D. Weightman and D. Appleton. "Data on the Distribution of Fibre Types in Thirty-six Human Muscles : An Autopsy Study." *J. neurolo scie.* 18, (1973): 111-129.
23. Kmenta, J. *Elements of Econometrics*. New York, Macmillan Publishing Co., Inc (1971).

24. Korner, L., P. Parker, C. Almstrom, P. Herberts and R. Kadefors, "The Relation Between Spectral Changes of the Myoelectric Signal and the Intramuscular Pressure of Human Skeletal Muscle". *Eur J Appl Physiol.* 52(2), (1984): 202-206.
25. Krivickas, L.S. "Power Analysis and Determination of Sample Size." *Lecture Notes.* Kessler Institute for Rehabilitation, (1994)
26. Krog-Lund, C., and K. Jergensen. "Changes in Conduction Velocity, Median Frequency, and Root Mean Square-Amplitude of the Electromyogram During 25% Maximal Voluntary Contraction of the Triceps Brachii Muscle, to Limit of Endurance." *Eur. J. Appl Physiol.* 63(1), (1991): 60-69.
27. Krog-Lund, C., and K. Jergensen. "Modification of Myo-electric Power Spectrum in Fatigue from 15% Maximal Voluntary Contraction of Human Elbow Flexor Muscles, to Limit of Endurance: Reflection of conduction Velocity Variation and/ or Centrally Mediated Mechanisms?" *Eur. J. Appl Physiol.* 64, (1992): 359-370.
28. Krog-Lund, C., and K. Jergensen. "Myo-electric Fatigue Manifestations Revisited: Power Spectrum, Conduction Velocity, and Amplitude of Elbow Flexor Muscles During Isolated and Repetitive Endurance Contractions at 30% Maximal Voluntary Contraction." *Eur. J. Appl Physiol.* 66, (1993): 161-173.
29. Kwatny, E., D.H. Thomas and H.G. Kwatny. "An Application of Signal Processing Techniques to the Study of Myoelectric Signals." *IEEE Trans Biomed Eng.* 17(4), (1970): 303-311.
30. Linssen, W. H.J.P., D.F Stegeman, E. M.G. Joosten, M.A. Van't Hof, R.A. Binkhorst, and S. L.H. Notermans. "Variability and Interrelationships of Surface EMG Parameters During Local Muscle Fatigue." *Muscle and Nerve.* (1993): 849-856.
31. Linssen, W. H.J.P., D.F Stegeman, E. M.G. Joosten, R.A. Binkhorst, M J.H. Merks, H.J. Ter Laak and S. L.H. Notermans. "Fatigue in Type I Fiber Predominance: A Muscle Force And Surface EMG Study on the Relative Role of Type I and Type II Muscle Fibers." *Muscle and Nerve.* (1991): 829-837.
32. Marieb, E.N. "Muscles and Muscle Tissue." *Human Anatomy and Physiology.* 2nd edition. California, The Benjamin/Cummings Publishing Company, Inc. (1992): 246-269.
33. McMahon, L.M., R.G. Burdett and S.L. Whitney. "Effects of Muscle Group and Placement Site on Reliability of Hand-Held Dynamometry Strength Measurements." *J. Orthop Sports Phys Ther.* 15(5), (1992): 236-242.

34. Merletti, R., M. Knaflitz, and C.J. De Luca. "Myoelectric Manifestations of Fatigue in Voluntary and Electrically Elicited Contractions." *J. Appl Physiol.* 69(5), (1990): 1810-1820.
35. Moritani, T., M. Muro and A. Nagata. "Electromyographic Manifestations of Muscular Fatigue." *Med Sci Sports Exer* 14(3), (1982): 198-202.
36. Moritani, T., M. Muro and A. Nagata. "Intramuscular and Surface Electromyogram Changes During Muscle Fatigue." *J. Appl Physiol.* 60(4), (1986): 1179-1185.
37. Neter, J and W. Wasserman. *Applied Linear Statistical Models*. Homewood, Richard D. Irwin, Inc (1974).
38. Nies, N., S. Richards and J. Asturias. "Intrarater and Interrater Reliability of Strength Measurements of the Biceps and Deltoid Using a Hand Held Dynamometer." *J Orthop and Sports Phys Ther.* 9(12), (1988): 399-405.
39. Proakis, J.G. and D.G. Manolakis. *Introduction To Digital Signal Processing*, New York, Macmillan Publishing Company (1990).
40. Riddle, D.L., S.D. Finucane, J.M. Rothstein and M.L. Walker. "Intrasession and Intersession Reliability of Hand-Held Dynamometer Measurements Taken on Brain-damaged Patients." *Phys Ther.* 69(3), (1989): 182-189.
41. Roy, S.J. "Combined Use of Surface Electromyography and ³¹P_NMR Spectroscopy for the Study of Muscle Disorders." *Phys Ther.* 73, (1993): 892:901.
42. Sloan, A.W. "Estimation of Body Fat in Young Men." *J. Appl Physiol.* 23, (1967): 311-315.
43. Solomonow, M., C. Batten, J. Smith, R. Baratta, H. Hermans, R. D'Ambrosia and H. Shoji. "Electromyogram Power Spectra Frequencies Associated with Motor Unit Recruitment Strategies." *J. Appl Physiol.* 68(3), (1990): 1177-1185.
44. Stashuk, D. and C.J. De Luca. "Median Frequencies of Cannula and Surface Detected Myoelectric Signals." *IEEE-EMBS Conference* (1987): 661:662.
45. Stulen, F.B and C.J. De Luca. "Frequency Parameters of the Myoelectric Signal as a Measure of Muscle Fiber Conduction Velocity." *IEEE Trans Biomed Eng.* 28, (1981): 515-523.
46. Sullivan, S.J., A. Chesley, G. McFaull and D. Scullion. "The Validity and Reliability of Hand-Held Dynamometry in Assessing Isometric External Rotator Performance." *J. Orthop Sports Phys Ther.* 10(6), (1988): 213-217.

47. Surburg, P.R., R. Sumoi, and W.K. Poppy. "Validity and Reliability of a Hand-Held Dynamometer with Two Populations." *J. Orthop Sports Phys Ther.* 16(5), (1992): 229-234.
48. Wadsworth, C.T., D.H. Nielsen, D.S. Corcoran, C.E. Phillips and T.L. Sannes. "Interrater Reliability of Hand-Held Dynamometry: Effects of Rater Gender, Body Weight, and Grip Strength." *J. Orthop Sports Phys Ther.* 16(2), (1992): 74-81.
49. Zwarts, M.J., T.W. Weerden and H.T.M. Haenen. "Relationship Between Average Muscle Fiber Conduction Velocity and EMG Power Spectra During Isometric Contraction, Recovery and Applied Ischemia." *Eur. J. Appl Physiol.* 56, (1987): 212-216.